

3 11

Reading File

BNWL-1229  
UC-80

**COBRA-II: A DIGITAL COMPUTER PROGRAM  
FOR THERMAL-HYDRAULIC SUBCHANNEL  
ANALYSIS OF ROD BUNDLE  
NUCLEAR FUEL ELEMENTS**

D. S. Rowe

February 1970

**AEC RESEARCH &  
DEVELOPMENT REPORT**

BNWL-1229

## LEGAL NOTICE

This report was prepared as an account of Government-sponsored work. Neither the United States, nor the Commission, nor any person acting on behalf of the Commission:

A. Makes any warranty or representation, expressed or implied, with respect to the accuracy, completeness, or usefulness of the information contained in this report, or that the use of any information, apparatus, method, or process disclosed in this report may not infringe privately owned rights; or

B. Assumes any liabilities with respect to the use of, or for damages resulting from the use of any information, apparatus, method, or process disclosed in this report.

As used in the above, "person acting on behalf of the Commission" includes any employee or contractor of the Commission, or employee of such contractor, to the extent that such employee or contractor of the Commission, or employee of such contractor prepares, disseminates, or provides access to, any information pursuant to his employment or contract with the Commission, or his employment with such contractor.

## PACIFIC NORTHWEST LABORATORY

RICHLAND, WASHINGTON

operated by

BATTELLE MEMORIAL INSTITUTE

for the

UNITED STATES ATOMIC ENERGY COMMISSION UNDER CONTRACT AT(45-1)-1830

3 3679 00061 6302

BNWL-1229

UC-80, Reactor  
Technology

COBRA-11: A DIGITAL COMPUTER PROGRAM  
FOR THERMAL-HYDRAULIC SUBCHANNEL ANALYSIS  
OF ROD BUNDLE NUCLEAR FUEL ELEMENTS

By

D. S. Rowe  
Fluid and Energy Systems Department  
Physics and Engineering Division

February 1970

BATTELLE MEMORIAL INSTITUTE  
PACIFIC NORTHWEST LABORATORIES  
RICHLAND, WASHINGTON 99352

This document is furnished pursuant to the Memorandum of  
Understanding of June 7, 1960, between U.S. and Canadian  
Governments, establishing a cooperative program on the  
development of heavy water moderated power reactors.

COBRA-PI may be obtained from the  
Argonne Code Center, 9700 South Cass Avenue  
Argonne, Illinois 60439

Printed in the United States of America  
Available from  
Clearinghouse for Federal Scientific and Technical Information  
National Bureau of Standards, U. S. Department of Commerce  
Springfield, Virginia 22151  
Price: Printed Copy \$3.00; Microfiche \$0.65

COBRA-II: A DIGITAL COMPUTER PROGRAM  
FOR THERMAL-HYDRAULIC SUBCHANNEL ANALYSIS  
OF ROD BUNDLE NUCLEAR FUEL ELEMENTS

D. S. Rowe

ABSTRACT

The COBRA-HI program calculates the steady-state flow and enthalpy in the subchannels of rod bundle nuclear fuel elements during both boiling and nonboiling conditions. The program uses a mathematical model that includes the effects of turbulent and diversion crossflow mixing between the subchannels. Turbulent crossflow mixing is caused by lateral flow fluctuations between subchannels and diversion crossflow mixing is caused by flow redistribution resulting from changes in the axial pressure gradient or from forced crossflow. The equations of the mathematical model are solved as an initial-value problem by using finite differences. The solution of the equations for flow, enthalpy, pressure and diversion crossflow must rely on input correlations to specify the turbulent crossflow and subchannel pressure gradient. The program is designed to allow the user to select these correlations to best fit his particular application. Besides having a faster and a more accurate numerical solution than in the original version of COBRA, COBRA-II has new features to improve its versatility. It can include the effect of subcooled voids. Subchannels may be typed so that nonuniform hydraulic behavior can be considered. Distorted bundles may be analyzed by selecting variable subchannel areas and gap spacings along the length. Spacer pressure loss and forced diversion crossflow can be considered. Turbulent mixing without boiling may be specified by several different correlation forms. During boiling, the mixing correlation for nonboiling can be used or turbulent mixing may be given as a function of steam quality. Adjustable dimensions are included in COBRA-II to allow the user to expand or contract the size of the program to accommodate his computer storage capability. The program has performed successfully with 36 subchannels, 25 fuel rods and 60 subchannel connections.

TABLE OF CONTENTS

<b>ABSTRACT</b>	iii
<b>INTRODUCTION</b>	1
<b>SUMMARY AND CONCLUSIONS</b>	1
<b>DESCRIPTION OF MATHEMATICAL MODEL</b>	3
<b>BASIC ASSUMPTIONS</b>	4
<b>GENERALIZED EQUATIONS</b>	4
Continuity	5
Energy	5
Axial Momentum	5
Transverse Momentum	5
<b>NUMERICAL SOLUTION</b>	7
Initial-Value Numerical Solution	7
Stability of the Initial-Value Solution	11
<b>COMPUTER PROGRAM DESCRIPTION</b>	13
<b>GENERAL FEATURES</b>	13
<b>PROGRAM ORGANIZATION</b>	14
<b>SUBROUTINES</b>	18
<b>USE OF COBRA</b>	22
<b>REFERENCES</b>	24
<b>NOMENCLATURE</b>	25
<b>APPENDIX A DERIVATION OF EQUATIONS</b>	A.1
<b>APPENDIX B GENERALIZED FORM OF THE EQUATIONS</b>	B.1
<b>APPENDIX C NUMERICAL STABILITY</b>	C.1
<b>APPENDIX D COMPUTER PROGRAM CORRELATIONS</b>	D.1
<b>APPENDIX E SAMPLE PROBLEM</b>	E.1
<b>APPENDIX F DISTRIBUTION</b>	F.1

COBRA-11: A DIGITAL COMPUTER PROGRAM  
FOR THERMAL-HYDRAULIC SUBCHANNEL ANALYSIS  
OF ROD BUNDLE NUCLEAR FUEL ELEMENTS

By

D. S. Rowe

INTRODUCTION

The purpose of this report is to describe the digital computer program, COBRA-II. This program is a refinement and extension of the earlier program COBRA<sup>(1)</sup> which was written to aid in calculating the flow and enthalpy in the subchannels of rod bundle nuclear fuel elements. COBRA-II contains many new features that make it a more flexible and useful tool for rod bundle subchannel analysis.

Subchannel analysis has become an important tool to help establish the thermal performance of rod bundle nuclear fuel elements because it considers the distribution of coolant flow and enthalpy in the bundle. This is a significant improvement over the bundle average analysis approach because the arrangement of fuel rods in present bundle design causes the local flow and enthalpy to be very different from the average. Subchannel analysis also allows better interpretation of laboratory data that give the thermal-hydraulic performance parameters such as critical heat flux and two-phase pressure drop. By using a subchannel analysis approach, the fuel designer can apply laboratory data to the reactor's operating conditions with a greater degree of confidence.

SUMMARY AND CONCLUSIONS

The digital computer program COBRA-11 computes the flow and enthalpy in the subchannels of rod bundle nuclear fuel during both boiling and nonboiling conditions. It uses a mathematical model that considers two types of cross-flow mixing. The first type is a net diversion crossflow caused by flow redistribution, and the second is a turbulent (fluctuating) crossflow caused by the random travel of coolant between adjacent subchannels. Each subchannel

is assumed to contain one dimensional, two-phase, slip-flow and is assumed to have a fine enough two-phase flow structure to permit specification of local void fraction as a function of enthalpy, flow, pressure and position. The equations of the mathematical model are solved as an initial-value problem by using finite differences. The numerical procedures are a significant improvement over the procedures used in the original COBRA program.

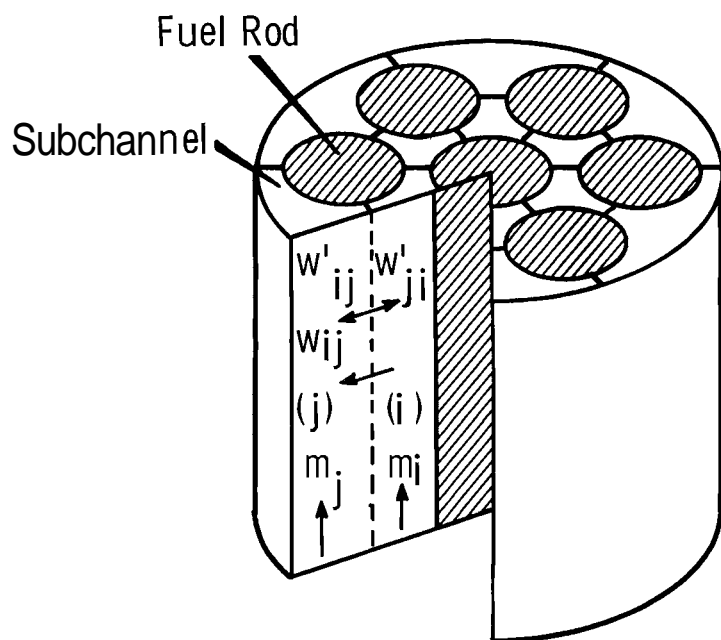
The COBRA-II program contains new features that permit analysis of many different rod bundle problems. Its significant features include the following:

- It has the ability to consider both single- and two-phase flow,
- It accounts for intersubchannel thermal mixing that results from thermal conduction, turbulent crossflow and diversion crossflow.
- It considers the momentum interchanges that result from both turbulent and diversion crossflow between adjacent subchannels,
- It includes the effect of transverse resistance to diversion crossflow.
- It can consider an arbitrary layout of fuel rods and flow subchannels and thus allows analysis of most any rod bundle configuration.
- It can include arbitrary heat flux distribution by specifying the axial flux distribution, relative rod power, and the fraction of rod power to each adjacent subchannel.
- It can consider variable subchannel area and gap spacings,
- It can include the effect of subcooled void.
- It can include the effect of forced diversion crossflow produced by flow diverting devices.
- It can include the pressure losses caused by spacing devices,
- It permits nonuniform hydraulic behavior by selecting different subchannel hydraulic characteristics.
- Input options are provided to allow the user to select various empirical correlations required for the calculations,

### DESCRIPTION OF MATHEMATICAL MODEL

Two-phase flow in rod bundle nuclear fuel elements is a complicated process which is not completely understood at the present time. One of the major difficulties is the inability to predict the transport processes of the liquid and vapor phases within the bundle. Reasonable descriptions of these processes have been made for selected regimes of two-phase flow in simple channels; but these descriptions cannot be easily applied to the complex geometry of rod bundles. This is because the added degrees of lateral freedom in rod bundles allows additional modes of liquid and vapor exchange which tend to invalidate the descriptions of transport processes in simple channels. This exchange, however, has a very significant influence on the flow and enthalpy in various regions of the bundle.

To develop a method for predicting the flow and enthalpy in selected regions of a rod bundle, a mathematical model is used that considers the important lateral transport processes. The approach used is essentially the same as in the original COBRA program where the cross section of the rod bundle is divided into discrete flow subchannels as shown in Figure 1.



By making suitable assumptions concerning the flow and crossflow in these subchannels, the equations of continuity, energy and momentum can be derived for each subchannel. This set of equations can then be solved numerically by using a digital computer.

#### BASIC ASSUMPTIONS

Steady, one-dimensional, two-phase flow exists in each subchannel during boiling.

- The two-phase flow structure is fine enough to allow specification of local void fraction as a function of enthalpy, pressure, flow rate and axial position
  - a A turbulent crossflow exists between adjacent subchannels that causes no net flow redistribution
  - a The turbulent crossflow may be superimposed upon a diversion crossflow between subchannels that results from flow redistribution. This may occur naturally by pressure gradients trying to equalize or may occur artificially from devices that force diversion crossflow
- Transverse spatial acceleration is neglected

#### GENERALISED EQUATIONS

The equations of continuity, energy, and momentum may be derived by using the basic assumptions as shown in Appendix 4. This derivation gives a set of  $3N$  first order, ordinary, differential equations plus  $K$  algebraic equations where  $N$  is the number of subchannels and  $K$  is the number of connections between subchannels. If the equations for flow, enthalpy and pressure are represented as  $N$  component column vectors and if the two crossflows are represented by  $K$  component column vectors, the transport equations may be written in the following matrix notation as shown in Appendix B.

Continuity

$$\left\{ \frac{dm}{dx} \right\} = -[R] \{w\} \quad (1)$$

Energy

$$\left\{ \frac{dh}{dx} \right\} = \{Q\} - [R][H]\{w^*\} - [R][T]\{c\} + [R][H^*]\{w\} \quad (2)$$

Axial Momentum

$$\left\{ \frac{dp}{dx} \right\} = -\{a\} - [R][U]\{f_T w^*\} + [R][U^*]\{w\} \quad (3)$$

Transverse Momentum

$$\{C|w|w\} = [S]\{p\} \quad (4)$$

The shorthand notation used in these equations gives a simple form that shows the basic phenomena included in the mathematical model. Now, consider the various terms in the above equations.

Equation (1) states that the rate of flow change in a subchannel is a linear combination of the diversion crossflows. The matrix transformation  $[R]$  is used to order only those crossflows permitted by the problem set up. The turbulent crossflow term does not appear in Equation (1) because, on a time average, it does not cause a net flow change.

In the Energy Equation (2), the terms on the right illustrate four mechanisms of thermal energy transport between the subchannels in a rod bundle fuel element. The first term  $\{Q\}$  is the power-to-flow ratio of a subchannel and gives the rate of enthalpy change if no thermal mixing occurs. The second term  $[R][H]\{w^*\}$  accounts for the turbulent enthalpy transport between all interconnected subchannels. This is analogous to eddy diffusion as discussed in Reference 1. The diagonal matrix  $[H]$  contains the subchannel

enthalpy differences for each pair of interconnected subchannels. The turbulent thermal mixing  $\{w^t\}$  is defined through empirical correlations. The third term  $[R][T]^c$  accounts for thermal conduction between adjacent subchannels. During boiling, the temperatures contained in  $[T]$  are limited to saturation temperature, therefore, the conduction term vanishes when all channels are boiling. The thermal conduction coefficient is defined in terms of geometric and fluid parameters. The fourth term  $[R][H^*]\{w\}$  accounts for thermal energy carried by the diversion crossflow. This is a convective term that requires a selection of the enthalpy to be carried by the diversion crossflow. This selection of the enthalpy is denoted by the matrix  $[H^*]$  which is set up the same way as  $[H]$ . The matrix  $[H^*]$ , however, permits selection of an effective enthalpy that is carried by the diversion crossflow. This may be used, for example, to account for the nonuniform enthalpy distribution in a subchannel by selecting the effective transported enthalpy from known information about the liquid-and vapor-phase distribution.

The right side of the Axial Momentum Equation (3) illustrates the mechanism of momentum transport. The first term  $\{a\}$  represents the pressure gradient without any crossflow between subchannels. It includes the friction, spatial acceleration and elevation components of pressure drop. This term gives the pressure gradient in an equivalent simple channel with the same thermal-hydraulic characteristics as the rod bundle subchannel. It is in this term where the important empirical correlations are contained that govern the subchannel flow solution. The second term  $[R][U]^t f_T \{w\}$  accounts for the turbulent momentum transport and is analogous to a Reynolds stress as discussed in Reference 1. The matrix  $[U]$  contains the subchannel velocities and is set up the same way as  $[H]$ . Since the analogy between thermal and momentum turbulent transport processes may not be the same, the factor  $f_T$  is included to modify the turbulent crossflow which is selected to satisfy the energy equation. The remaining term  $[R][U^*]\{w\}$  of Equation 43) is the momentum contribution of the diversion crossflow. This is a convective term that is analogous to the convective energy term. The matrix  $[U^*]$  contains the axial velocities that are carried through the gap by the diversion crossflow.

The Transverse Momentum Equation (4) is a simple friction model where the pressure drop between subchannels is proportional to the diversion crossflow rate squared. The resistance coefficient  $C$  is evaluated in terms of an empirical function which depends on the geometric and flow parameters. This equation has rather weak influence for a few problems, but it plays an important role in the numerical stability of some solutions.

#### NUMERICAL SOLUTION

The flow in rod bundle subchannels is governed by the boundary conditions imposed at the ends of the bundle; therefore, the flow solution requires a boundary-value solution. Since this solution is difficult to set up and difficult to solve, a simpler initial-value solution is commonly accepted as an approximate solution. Various types of initial-value solutions are used in the HAMBO<sup>(2)</sup>, SASS<sup>(3)</sup>, THINC-II<sup>(4)</sup> and MIXER<sup>(5)</sup> sub-channel analyses programs.

The use of an initial-value solution can be justified from the results presented in Reference 6 where an initial-value solution is shown to adequately approximate the boundary-value solution if a stability criterion is satisfied. This criterion gives the minimum allowable calculation increment in terms of the crossflow resistance. The actual calculation increment must be larger than this to permit proper flow redistribution. If the increment is smaller than this, the flow redistribution occurs over additional calculation increments, and a boundary-value solution is required.

The numerical procedure in COBRA-II uses an initial-value solution that is patterned after the one discussed in Reference 6. By applying this procedure to many subchannels, a similar set of numerical equations and a similar stability criterion is obtained.

#### Initial-Value Numerical Solution

Equations (1) through (4) are solved as an initial-value problem by using finite differences. It is assumed that the values of  $\{m\}$ ,  $\{h\}$ ,  $\{w\}$  and  $\{p\}$  are available to start the solution. Both forward and backward

finite differences are used for the solution. The Energy Equation (2) is solved by using the forward difference equation

$$\left\{ \frac{h(x+\Delta x) - h(x)}{\Delta x} \right\} = \{Q(x)\} + [R][T(x)]\{C(x)\} - [R][H(x)]\{w^*(x)\} + [R][H^*(x)]\{w(x)\} \quad (5)$$

This equation can be easily solved for  $\{h(x+\Delta x)\}$  because all other quantities are known. A backward finite difference is used to solve the Continuity and Momentum Equations. For the Continuity Equation (1) the difference equation is

$$\left\{ \frac{m(x+\Delta x) - m(x)}{\Delta x} \right\} = -[R]\{w(x+\Delta x)\}. \quad (6)$$

The values of  $\{w(x+\Delta x)\}$  must be obtained before this equation can be solved for  $\{m(x+\Delta x)\}$ . An equation for  $\{w\}$  can be obtained by eliminating pressure from Equations (3) and (4). The result\*\* is

$$\frac{d(C|w|w)}{dx} = -[S]\{a^*\} + [S][R][U^*]\{w\} \quad (7)$$

$$\text{where } \{a^*\} = \{a\} + [R][U]\{f_T w^*\} \quad (8)$$

The backward difference approximation is used in this equation which gives

$$\left\{ \frac{C(x+\Delta x)|w(x+\Delta x)|w(x+\Delta x) - C(x)|w(x)|w(x)}{\Delta x} \right\} = [S]\{a^*(x+\Delta x)\} + [S][R][U^*(x+\Delta x)]\{w(x+\Delta x)\}. \quad (9)$$

\*The use of the backward difference eliminates the confusing crossflow sign inconsistency in the original COBRA program.

\*\*Notice that Equation (7) could be differentiated again and after substituting Equation (1) would give a system of second order equations that could be solved as a boundary-value problem for  $\{w\}$ ,

By substituting Equation (4) and rearranging, this may be written as

$$\left[ \frac{C(x+\Delta x) |w(x+\Delta x)|}{\Delta x} + [S][R][U^*(x+\Delta x)] \right] (w(x+\Delta x)) = [S]\{a'(x+\Delta x)\} + \frac{1}{\Delta x}[S]\{p(x)\} \quad (10)$$

Equation (10) is a set of  $K$  simultaneous, nonlinear equations and  $K$  unknowns. This can be solved as a linear system by iteration where, for each iteration, the previous iterate is used for  $\{C(x+\Delta x) |w(x+\Delta x)| / \Delta x\}$ ,  $[U^*(x+\Delta x)]$  and  $\{a'(x+\Delta x)\}$ . Once the iterative solution for  $\{w(x+\Delta x)\}$  converges to within an acceptable tolerance,  $\{m(x+\Delta x)\}$  can be calculated from Equation (6) and  $\{p(x+\Delta x)\}$  can be calculated from

$$\left\{ \frac{p(x+\Delta x) - p(x)}{\Delta x} \right\} = -\{a'(x+\Delta x)\} + [R][U^*(x+\Delta x)]\{w(x+\Delta x)\} \quad (11)$$

which is a backward difference approximation to Equation (3).

The procedure used to solve these equations is patterned after the iterative solution contained in Reference 6, and it is illustrated in Figure 2. Initial values of  $\{h(x)\}$ ,  $\{m(x)\}$ ,  $\{w(x)\}$  and  $\{p(x)\}$  are first established. Equation (5) is used to calculate  $\{h(x+\Delta x)\}$ . The values of  $\{m(x)\}$ ,  $\{w(x)\}$  and  $\{p(x)\}$  are assumed to apply at  $x+\Delta x$  for the purpose of evaluating fluid properties. With this information, the liquid and two-phase properties can be evaluated at  $x+\Delta x$ . In the present writing of COBRA, these properties are assumed\* to remain constant for the iteration loop that follows.

The iteration loop starts by using the fluid properties to evaluate  $\{C(x+\Delta x) |w(x+\Delta x)| / \Delta x\}$ ,  $\{a'(x+\Delta x)\}$  and  $\{U^*(x+\Delta x)\}$ ; then,  $\{w(x+\Delta x)\}$  is calculated by using Equation (10). The new  $\{w(x+\Delta x)\}$  is compared with the old one to determine if all of the crossflows have converged to within an

---

\*Fluid property evaluation could be included in the iteration loop, but it can cause instabilities near the point of boiling when void correlations are used that depend on flow rate.

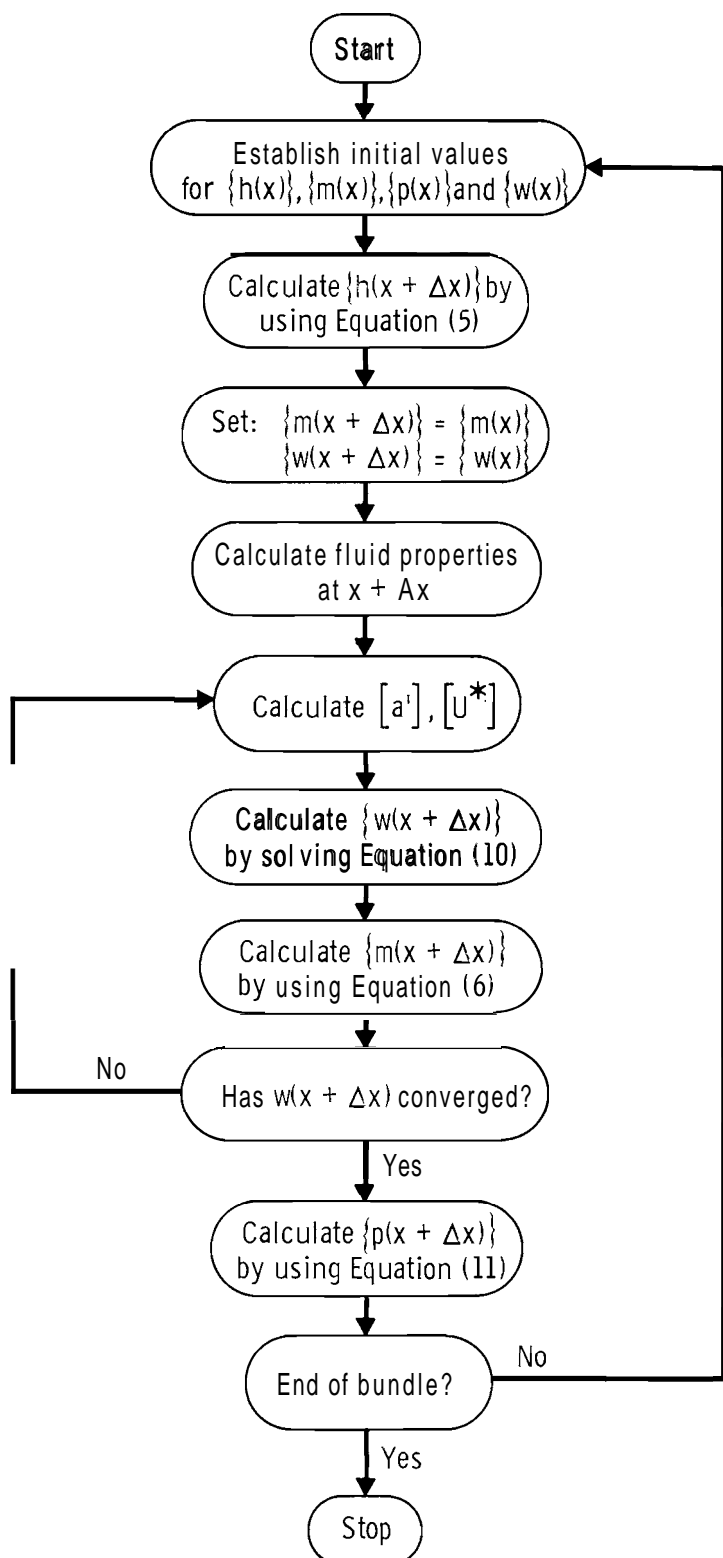


FIGURE 2. Initial-Value Solution

acceptable tolerance. If convergence does not occur, a signal is set up to remain in the loop for another iteration. Since the new solution for  $\{w(x+\Delta x)\}$  is quite sensitive to the old one,  $\{w(x+\Delta x)\}$  is modified by

$$\{w(x+\Delta x)\} = \frac{1}{2} \{w(x+\Delta x)\}_{\text{calc}} + \frac{1}{2} \{w(x+\Delta x)\}_{\text{old}} \quad (12)$$

This value is then used in Equation (6) to calculate  $\{m(x+\Delta x)\}$  which is used in the next iteration if convergence did not occur. If convergence did occur,  $\{p(x+\Delta x)\}$  is calculated from Equation (11) and the calculation moves to the next increment,

#### Stability of the Initial-Value Flow Solution

The backward difference is used in Equation (7) because of severe stability limitations that are required with a forward difference. If Equation (7) is pre-multiplied by a matrix  $[C^{-1}]$  with only diagonal elements of  $1/C$ , the following equation is obtained

$$\left\{ \frac{d|w|}{dx} \right\} = -[C^{-1}] [S] \{a^*\} + [C^{-1}] [S] [R] [U^*] \{w\} \quad (13)$$

The elements of  $[S]$ ,  $[R]$  and  $[U^*]$  are of the order unity, but the elements of  $[C^{-1}]$  can be many orders higher. Therefore, the eigenvalues of the characteristic matrix of Equation (13) are very large. As shown in Appendix C, a stable solution for such a set of equations is not possible with a forward difference. By using a backward difference approximation for the flow solution, stable solutions can be obtained if two requirements are satisfied. The first requires that there be a sufficiently large crossflow resistance to prevent transverse flow loops, and the second requires a significantly large  $\Delta x$  for a given crossflow resistance. These two requirements will now be discussed.

Equation (10) may be written more compactly as

$$[A] \{w(x+\Delta x)\} = \{B\}. \quad (14)$$

This is a set of  $K$  simultaneous equations and  $K$  unknowns. A solution is possible if  $[A]$  is not singular. It should be noted that  $[A]$  is the matrix  $-[S][R][U^*]$  but with its diagonal elements modified by adding the diagonal matrix  $[C|w|/\Delta x]$ . For any rod bundle problem that has one or more flow paths around a fuel rod (or any transverse flow loop) the matrix  $-[S][R][U^*]$  is singular and only by adding  $[C|w|/\Delta x]$  does it become nonsingular. Physically, the addition of this term means that the summation of pressure drops around any transverse flow loop must be zero. The problem is that these added diagonal elements are small as compared to the nonzero elements of  $[S][R][U^*]$ ; therefore,  $[A]$  can be close to singular for some problems. Fortunately, there is control over this by selecting a sufficiently small step size for a given crossflow resistance coefficient, provided the value of  $|w|$  is not zero. To eliminate the problem of  $|w|$  going to zero, the crossflow resistance is linearized for small values of crossflow in the present writing of COBRA. This is done by putting a lower limit on  $|w|$ ; thus, for  $w = w_L$ ,  $|w| = w_L$  and for  $|w| > w_L$ ,  $|w| = |w|$ .

In addition to requiring that  $[A]$  be nonsingular, the second requirement is that the absolute value of the largest eigenvalue of  $[A]^{-1}$  must be less than one (see Equation (14)). This criterion puts a power limit on the calculation increment for a given crossflow resistance. Its physical basis, which is discussed in Appendix C and Reference (6), requires that the diversion crossflow occur within the increment  $\Delta x$  and still satisfy the momentum equations. If this condition is not satisfied, errors grow in the flow solution and flow reversals may occur in an attempt to satisfy the momentum equations. Fortunately, the minimum  $\Delta x$  is much smaller than the  $\Delta x$  desired for most rod bundle calculations.

The previous discussion helps to clarify the role of the crossflow resistance in the COBRA-II program. Notice that in Equations (7) and (10) the crossflow resistance terms are very small, thus, the crossflows are driven by differences in the axial pressure gradient. The crossflow resistance should be interpreted as a mechanism that directs the diversion

crossflow through the path of least resistance and gives zero pressure drop around transverse flow loops. The crossflow resistance only has importance when these loops exist. For problem where there are no loops, the crossflow resistance has little importance because the stability criterion requires dominance of  $[S][R][U^*]$  over  $[C|w|/\Delta x]$ .

#### COMPUTER PROGRAM DESCRIPTION

The COBRA-II program is a revised version of the original COBRA program. This revision has been guided by **users' comments** and through experience which has identified the need for improvements and expanded capability. This has resulted in a rather general program that can be used by the nuclear industry for analysis of many rod bundle **thermal-hydraulics** problems.

COBRA-II should be thought of as an automated solution to the basic set of differential equations of the mathematical model. To actually perform this solution, the user must provide input. This input not only includes the geometric parameters and operating conditions but also the various required empirical or **semiempirical** correlations. Any set of **correlations** can give a solution, but some correlations will give better **solutions**. At the **present** time, guidelines have not been established for complete selection of these correlations; therefore, the COBRA-II program does not contain a **pre-selected** set of input correlations. Several correlations are provided for examples, but the final selection must be made by the user,

The following **sections** present the general features of the COBRA-II program, **an** illustrated description of the program organization and a description of the **program's** subroutines,

#### GENERAL FEATURES

The significant features of COBRA-II **include** the following:

- It has **the** ability to consider both single- and two-phase flow,
- It can consider the effects of turbulent and thermal conduction mixing throughout **the** bundle by using empirically determined mixing coefficients,

- It includes mixing which results from the convective transport of enthalpy by diversion crossflow.
- It includes the momentum transport between adjacent subchannels which results from both turbulent and diversion crossflow,
- It includes the effect of transverse resistance to diversion crossflow,
- It can consider an arbitrary layout of fuel rods and flow subchannels for analysis of most *any* rod bundle configuration. A single subchannel may interact with up to four adjacent subchannels, and a fuel rod may transfer heat to a maximum of six adjacent subchannels.
- It can include arbitrary heat flux distribution by specifying the axial flux distribution, relative rod power, and the fraction of rod power to each of the six adjacent subchannels. (The latter feature allows variation in circumferential rod heat flux.)
- It can consider variable subchannel area and gap spacing,
- It can consider forced diversion crossflow by specifying the local diversion crossflow in terms of geometric and flow parameters.
- It can consider nonuniform hydraulic behavior by assigning different single-phase friction factors to selected subchannels.
- Its subroutines are designed to allow the user to set up empirical correlations of his choice and then select these correlations through input options.
- It includes options to select the inlet flow and enthalpy conditions,

#### PROGRAM ORGANIZATION

The organization of the COBRA II program is similar to that of the original COBRA program; however, the input procedures and subroutines have been reorganized to permit the expanded program capability. The calculational procedures have also been revised to use the previously described numerical solution.

The organization of the program can best be described by following the flow chart of Figure 3. The first function of the program is to read in the input data. This is accomplished by successively reading in the 12 groups of input data that are required for the calculations. Some of these groups are optional and are not needed for certain problems. New cases, after the first, require input of only the card groups that will change the input of the previous case,

Following the input, the initial conditions are established. Previously stored values of initial conditions of inlet flow, enthalpy and pressure are recalled or the initial conditions are established from new input data. Subroutine SPLIT is used here to calculate subchannel flows to give equal subchannel pressure gradients if it is requested by an input option,

The new input data for each case may be printed out prior to starting the calculations. The user can also omit this or can print out the entire set of input for each case,

A loop is now entered which takes the calculation stepwise through the bundle at preselected steps of  $\Delta x$ . At the beginning of selected steps, the answers are saved for later printing. When the end of the bundle is reached, these answers are printed as specified by options,,

At the beginning of each space step, the rate of enthalpy rise  $\{dh/dx\}$  is calculated in Subroutine DIFFER(1) and this is used to calculate  $\{h(x+\Delta x)\}$ . Properties are evaluated at  $x+\Delta x$  by using  $\{m(x)\}$ ,  $\{w(x)\}$  and the reference pressure. All geometries and flow parameters are now calculated at  $x+\Delta x$  by using Subroutines AREA, FORCE, PROP(2), VOID and MIX,

An iteration loop is now started to refine the previous estimates of  $\{m(x+\Delta x)\}$  and  $\{w(x+\Delta x)\}$ . In this iteration, the previously estimated flow properties are assumed to be sufficiently accurate that the iteration may proceed without their continual re-evaluation. For problems where this assumption is not valid, the property evaluation could be easily included for each iteration. The values of  $\{a^*(x+\Delta x)\}$  and  $[S][R][U^*(x+\Delta x)]$  are

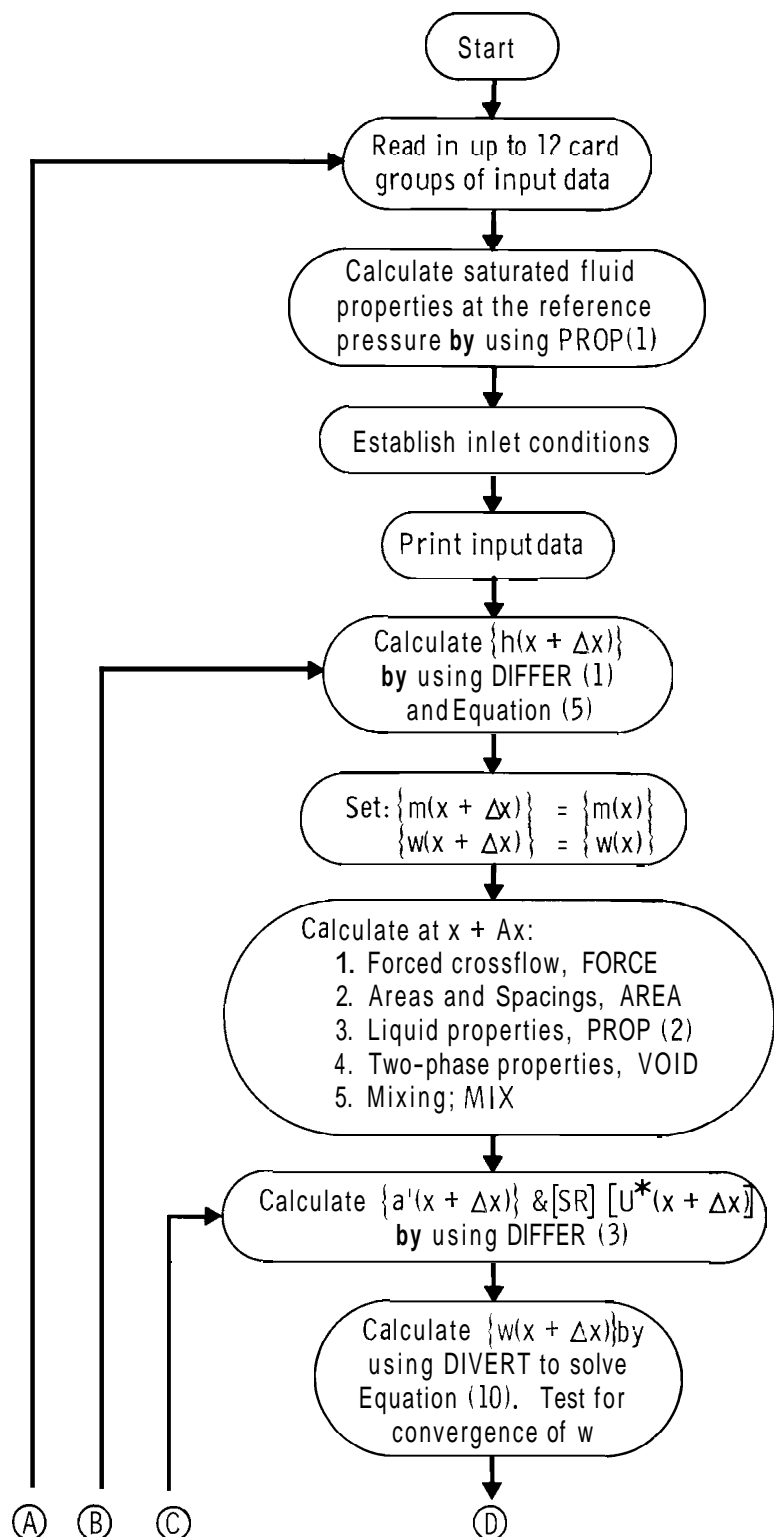


FIGURE 3. COBRA-II Flow Diagram

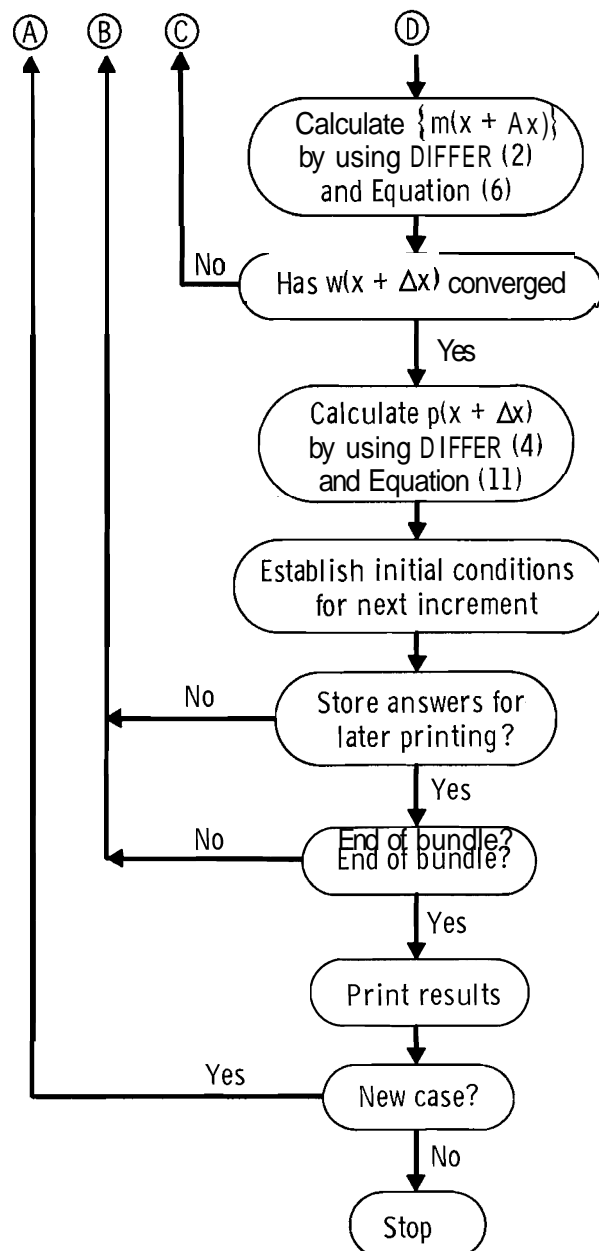


FIGURE 3. COBRA-II Flow Diagram (Contd.)

evaluated by using Subroutine DIFFER(3) for each iteration because they are flow dependent. With these quantities defined, Equation (14) can be solved for  $\{w(x+\Delta x)\}$  by using DIVERT. Now, by using Subroutine DIFFER(2),  $\{dm/dx\}$  is calculated and then  $m(x+\Delta x)$  is calculated by using Equation (6). When  $\{w(x+\Delta x)\}$  converges to within an acceptable tolerance, the iteration is stopped and a calculation of  $\{dp/dx\}$  is made using Subroutine DIFFER(4), and this is used to calculate  $\{p(x+\Delta x)\}$  by using Equation (11). The initial conditions are now established for the next increment?

### SUBROUTINES

The organization of the COBRA-II program puts most of the calculational effort into subroutines. The more important ones will now be discussed to describe their function and to identify the required input correlations,

#### Subroutine DIFFER(IPART)

This subroutine is used to calculate the spatial derivatives of flow, enthalpy and pressure. It is divided into four parts as indicated by the variable IPART. The notation and procedures used in DIFFER do not correspond directly to the notation used in the previously presented matrix equations. There are actually no rectangular matrices  $[R]$ ,  $[S]$ ,  $[U^*]$ , etc. There are, however, the column vectors corresponding to  $\{w^*\}$ ,  $\{C\}$ ,  $\{w\}$ ,  $\{m\}$ ,  $\{h\}$ ,  $\{p\}$  and  $\{a^*\}$  which are defined in the Nomenclature. The method of performing the previously indicated matrix transformations is actually done by using the index notation of Appendix A and the subchannel connection scheme presented in Appendix B. As an example of how this is done, the calculation performed in the second part of Subroutine DIFFER will be explained in detail,

In this calculation, the elements of  $\{dm/dx\}$  are calculated by using Equation (A-3) which as

$$\frac{dm_i}{dx} = \sum_{j=1}^N w_{ij} \quad i = 1, 2, \dots, N_c \quad (A-3)$$

By using the subchannel connection notation of Appendix B, each pair (ij) gives a subchannel connection number k that is identified by the array KCHAN(I,J). If there is no connection KCHAN(I,J) is zero. The values of  $\frac{dm_i}{dx}$  are calculated by selecting a subchannel number (i) and then, by considering all other subchannels (j), accumulate those values of  $w_k$  that have nonzero values of k. To account for the direction of the diversion crossflow the sign of  $w_k$  is positive if  $i < j$  and is negative if  $i > j$ . This procedure is equivalent to performing the transformation  $[\mathbf{R}]\{w\}$ .

The calculation of the other spatial derivatives is done in much the same way. Some explanation is required, however, to show how  $[U^*]$  and  $[H^*]$  are treated. These quantities include the axial velocity and enthalpy that are transported through the gap by the diversion crossflow. Since they are both handled the same way, consider  $[H^*]$ . From Appendices A and 13, the elements of  $[\mathbf{R}][H^*]\{w\}$  are

$$\sum_{j=1}^N (h_i - h^*) \frac{w_{ij}}{m_i} \quad i = 1, 2, \dots, N$$

where  $h^*$  is presently defined in COBRA-II as

$$h^* = \begin{cases} h_i; & \text{if } w_{ij} \geq 0 \\ h_j; & \text{if } w_{ij} < 0 \end{cases}; \quad (15)$$

therefore, the enthalpy being carried through the gap by the diversion crossflow is the enthalpy from the donor subchannel. Similarly

$$u^* = \begin{cases} u_i; & \text{if } w_{ij} \geq 0 \\ u_j; & \text{if } w_{ij} < 0 \end{cases}. \quad (16)$$

Both Equations (15) and (16) imply that the enthalpy and velocity are uniform in each subchannel. In reality, this is an approximation. As additional information is obtained concerning two-phase transport processes in bundles  $h^*$  and  $u^*$  can be formulated more correctly,

#### Subroutine DIVERT

This subroutine sets up Equation (14)

$$[A]\{w(x+\Delta x)\} = \{B\} \quad (14)$$

and solves for  $\{w(x+\Delta x)\}$ . The setup is done by using **index** notation and not actually by using the matrices  $[S]$ ,  $[R]$  and  $[U^*]$ . This setup uses  $\{a^i\}$  and the coefficients of  $\{w\}$  which are calculated in DIFFER(3). The elements of  $[A]$  are filled by successively selecting rows from which the pair of adjacent subchannels can be defined by the arrays  $IK$  and  $JK$ . Each element of the **row** is then filled to correspond to the subchannel connection logic.

If forced flow diversion between subchannels is specified by **FORCE** Equation (14) is modified to account for this. After the modification is complete, Equation (14) is solved for  $\{w(x+\Delta x)\}$ .

#### Subroutine MIX

Subroutine **MIX** calculates the thermal mixing parameters that are vital to subchannel analysis. This includes both the turbulent and thermal conduction mixing coefficient. Since completely acceptable correlations for mixing have not been developed for single and two phase mixing, this subroutine is set up so that improved correlation functions can be included when they become available. The approach used for now is to separate the mixing into boiling and nonboiling regions. For nonboiling conditions, several correlation forms are included as shown in Appendix D. For two-phase flow, the single-phase correlations may be assumed to apply or the mixing rate may be specified as a function of quality,

The thermal conduction coefficient is assumed to be a function of the **subchannel** geometry and the average fluid **thermal** conductivity as shown in Appendix D.

#### Subroutine PROP(IPART)

This subroutine consists of two parts. The first part calculates the saturated fluid properties as a function of the system reference pressure, The second part calculates all the liquid fluid properties as a function of **temperature** and **limits** these to saturated values during **boiling**. The second part also **calculates** the convection heat transfer coefficient and the **single-phase** friction factor with a wall viscosity correction,

#### Subroutine VOID

Subroutine **VOID** **calculates** the two-phase flow **parameters** which include **subcooled** void fraction, bulk void fraction, **density**, effective specific volume for **momentum** and **two-phase** friction gradient multiplier, Several correlations are included in this subroutine that the user can select by option, These are provided as an example with the thought that the users will set up correlations that are most **applicable** to their particular problems,

#### Subroutine AREA

This subroutine **calculates** **subchannel** area and gap **spacings** by using the tabular list of area and gap **variations** supplied as **input**. A linear interpolation is used to select values from *these* tables,

#### Subroutine FORCE

Subroutine **FORCE** is provided to specify forced diversion crossflow at selected gaps and at selected axial positions, If a forced crossflow is specified, the logical variable **FDIV** = .TRUE.; otherwise, **FDIV** = .FALSE. An example of how forced **crossflow** is treated is included in the present writing of COBRA, In this example, flow diverters may be assigned to spacers which divert a fraction of the flow out a **subchannel** into another one, This flow fraction is converted into a diversion **crossflow** per unit length by dividing the diverted flow by  $\Delta x$ .

### Other Subroutines

Several other subroutines are required for operation of the COBRA-II program. Subroutine CURVE performs a linear interpolation of tabulated data, Subroutine DECOMP and SOLVE perform the solution to the simultaneous equations, Subroutine SPLIT divides the subchannel flow rates at the inlet of the bundle to give equal pressure gradients by assuming that there is no spatial acceleration component of pressure drop.

### USE OF COBRA

The COBRA-II program is written for the WIVAC-1108. Except for the round-off problem that are encountered on computers with a short word length, there should be no difficulty in setting up and operating this program for other computers capable of compiling FORTRAN IV or V. Adjustable dimensions are included so that the program can be easily contracted or expanded to accomodate the users computer or problem size,

Complete input instructions are included in the program listing. A sample problem that illustrates the input and use of the new features of COBRA-II is given in APPENDIX E. The input is set up with options by which the user may select correlations for input to a problem. This has been done to make it clear that the user should treat these correlations as input since none of these correlations have universal validity. By forcing the user to make this selection, the correlations are given the status of input. In particular, the user must select or provide for:

- Friction factor correlation
- Subcooled void fraction correlation
- Two phase friction multiplier correlation
- Two-phase void fraction correlation
- Single-phase mixing correlation
- Two-phase mixing correlation
- Pressure loss coefficients for spacers
- Flow diversion from spacing devices
- Diversion crossflow resistance factor

Many of these **correlations** already exist from studies of flow in simple channels; however, there is not yet enough **information** to indicate which correlations are best for most rod bundle **problems**. An evaluation of available correlations will have to be made to **determine** which correlations are suitable for rod bundle subchannel analysis,

REFERENCES

1. D. S. Rowe. Crossflow Mixing Between Parallel Flow Channels During Boiling, Part I, COBRA--Computer Program for Coolant Boiling in Rod Arrays, BNWL-371, Pt 1. Pacific Northwest Laboratory, Richland, Washington (March 1967).
2. R. W. Bowring. HAMBO, A Computer Programme for the Subchannel Analysis of the Hydraulic and Burnout Characteristics of Rod Clusters, Part 1, General Description, AEEW-R524. Atomic Energy Establishment, Winfrith, Great Britain (1967).
3. C. C. St. Pierre. SASS Code 1, Subchannel Analysis for the Steady State, AECL-APPE-41. Atomic Energy of Canada, Ltd., Chalk River, Ontario, Canada (1966).
4. Proprietary Computer Program of Westinghouse Electric Co., Pittsburgh, Pennsylvania.
5. Proprietary Computer Program of General Electric Co., San Jose, Calif California.
6. D. S. Rowe, "Initial-and Boundary-Value Flow Solutions During Boiling in Two Interconnected Parallel Channels," American Nuclear Society Transactions, Vol. 12, No. 2, pp 834-835 (November 1969).
7. J. E. Meyer. Conservation Laws in One-Dimensional Hydrodynamics, WAPD-BT-20, pp. 61-72. Westinghouse Electric Corporation, Bettis Atomic Power Laboratory, Pittsburgh, Pennsylvania (September 1960).
8. J. P. Waggener. "Friction Factors for Pressure Drop Calculations," Nucleonics, Vol. 19, p. 145 (1961).
9. L. S. Tong. "Pressure Drop Performance of a Rod Bundle," Heat Transfer in Rod Bundles, ASME, pp. 57-69 (1968).
10. A. A. Armand. "The Resistance During the Movement of a Two-Phase System in Horizontal Pipes," Translated by V. Beak, AERE Trans, 828. Izvestiya Vsesojuzного Teplotekhnicheskogo Instituta (1), pp. 16-23 (1946).
11. W. A. Massena. Steam-Water Pressure Drop and Critical Discharge Flow - A Digital Computer Program, HW-65706. Hanford Atomic Products Operation, Richland, Washington (June 17, 1960).
12. S. Levy. Forced Convection Subcooled Boiling--Prediction of Vapor Volumetric Fraction, GEAP-5157. General Electric Co., Atomic Power Equipment Dept., San Jose, California (April 1966).
13. J. T. Rogers and N. E. Todreas. "Coolant Mixing in Reactor Fuel Rod Bundles--Single-Phase Coolants," Heat Transfer in Rod Bundles, ASME, pp. 1-56 (1968).
14. D. S. Rowe and C. W. Angle. Crossflow Mixing Between Parallel Flow Channels During Boiling, Part III, Effect of Spacers on Mixing Between Two Channels, BNWL-371, Pt. 3. Pacific Northwest Laboratory, Richland, Washington (January 1969).

NOMENCLATURE\*

<u>Equations</u>	<u>Computer Program</u>	
$a$	DP	Single channel pressure gradient
$a'$	DP	Pressure gradient without crossflow in Equation (3), $(F/L^3)$
$A$	A	Cross-sectional area, $(L^2)$
$[A]$	AAA	Matrix of coefficients in Equation (14)
$\{B\}$	B	Column vector in Equation (14)
$c$	COND	Thermal conduction coefficient'. $(H/T\theta)$
$C$	C	Loss coefficient for transverse crossflow in Equation (4)
$C_p$	CP	Specific heat $(H/M\theta)$
$dh/dx$	DH	Enthalpy derivative, $(H/L)$
$dm/dx$	DF	Flow derivative, $(M/TL)$
$dp/dx$	DP	Pressure derivative $(F/L^3)$
$D$	DHYD	Hydraulic diameter, $4A/P_w$ , $(L)$
$D_r$	D	Rod diameter $(L)$
$f$	FSP	Friction factor based on all-liquid flow, (Dimensionless)
$f_A$	AXIAL	Local to average axial power distribution (Dimensionless)
$f_c$	PWRF	Fraction of rod power transferred to an adjacent subchannel (Dimensionless)
$f_\ell$	FL	Uivcresion crossflow resistance parameter $(L)$
$f_R$	RADIAL	Relative roil power distribution (Dimensionless)
$f_T$	FM	Turbulent momentum factor (Dimensionless)

---

\*Dimensions are denoted by:

$L$  = length,  $T$  = time,  $M$  = mass,  $\theta$  = temperature,  
 $F$  =  $ML/T^2$  = force and  $H$  =  $ML^2/T^2$  = energy

<u>Equations</u>	<u>Computer Program</u>	
F		Force (ML/T <sup>2</sup> )
$g_c$	G	Gravitational constant, (ML/FT <sup>2</sup> )
G		Mass velocity, (M/TL <sup>2</sup> )
h	HFILM	Heat transfer coefficient, (H/TL <sup>2</sup> θ)
h	H	Enthalpy, $Xh_g + (1-X)h_f$ , (H/M)
$h^*$	HSTAR	Enthalpy carried by diversion crossflow, (H/M)
$h_g, h_f$	EG,IIF	Saturated vapor and liquid enthalpy (H/M)
[H], [H*]		Enthalpy matrices defined by Equations (B=6) and (B=7), (HT/M <sup>2</sup> )
k	CON	Thermal conductivity, (H/TLθ)
K	NK	Number of connections between adjacent subchannels, [Dimensionless]
K	CDRAG,CD	Spacer loss coefficient
$K_g$	GK	Geometry factor for conduction (Dimensionless)
l		Length, (L)
L	Z	Channel length, (L)
m	F	Mass flow rate, $Au_f[\rho g \alpha + \rho_f(1-\alpha)]$ , (M/T)
N	NCHANL	Number of subchannels [Dimensionless]
p		Pressure (F/L <sup>2</sup> )
$P_H$	HPERIM	Heated perimeter, (L)
$P_w$	PERIM	Wetted perimeter, (L)
$P_r$	PRANTL	Prandtl number (Dimensionless)
$q^i$	QPRIM	Heat addition per unit length, (H/L)
$\bar{q}'$	AFLUX	Average heat flux, (H/TL <sup>2</sup> )
Q		Specific power to-flow ratio, $q_i^i/m_i$ , (H/ML)
Q	Q	Parameter given by Equation (D-17)
[R]		Matrix to order crossflows (Dimensionless)
Re	RE	Reynolds number, (Dimensionless)

<u>Equations</u>	<u>Computer Program</u>	
$s$	GAP	Rod spacing (L)
$[S]$		Matrix transformation defining adjacent subchannels, (Dimensionless)
$t$	T	Temperature ( $\theta$ )
$u$	U	Channel effective momentum velocity
$u^*$	USTAR	Effective velocity carried by diversion crossflow (L/T)
$[U]$		Velocity matrix defined by Equation (B-11), ( $T/L^2$ )
$[U^*]$	DD	Velocity matrix defined by Equation (B-12), ( $T/L^2$ )
$v$	V	Liquid specific volume, $1/\rho$ , ( $L^3/M$ )
$v'$	VP	Effective specific volume for momentum, $(1-X)^2/\rho_f(1-\alpha) + X^2/\rho_g\alpha$ , ( $L^3/M$ )
$w$	W	Diversion crossflow between adjacent subchannels (M/TL)
$w'$	WP	Turbulent (fluctuating) crossflow between adjacent subchannels, (M/TL)
$x$	X	Distance (L)
$X$	QUAL	Quality, $m_g/(m_g + m_f)$ , (Dimensionless)
$X_d$	XD	Parameter given by Equation (D-15)
$Y_B$	YB	Parameter given by Equation (D-19)
$z_{ij}$	LENGTH	Effective centroid distance (L)
$\alpha$	ALPHA	Void fraction, $A_g/(A_g + A_f)$ , (Dimensionless)
$\beta$	BETA	Turbulent mixing parameter, (Dimensionless)
$\gamma$	AV(1)	Slip ratio, $u_g/u_f$ , (Dimensionless)
$\theta$	THETA	Orientation of channel with respect to vertical, (Radians)
$\rho$	RHO	Density, $\rho_g\alpha + \rho_f(1-\alpha)$ , ( $M/L^3$ )

<u>Equations</u>	<u>Computer Program</u>	
$\rho_g, \rho_f$	RHOG, RHOF	Saturated vapor and liquid density, (M/L <sup>3</sup> )
$\sigma$	SIGMA	Surface tension, (F/L)
$\tau_w$	TAUW	Wall shear stress (F/L <sup>2</sup> )
$\phi$	PHI, FMULT	Two-base friction multiplier, (Dimensionless)
$\mu$	VISC	Viscosity, (F/LT)

Subscripts

$f, g$		Saturated conditions for liquid and vapor, respectively
$i, j$	$i, j$	Channel identification number
$ij, ji$		Double subscripts imply $i$ to $j$ and $j$ to $i$ , respectively
$k(i, j)$	KCHAN	Number identifying each subchannel connection; each $k$ implies a pair $ij$ or $ji$
$r$		Rod identification number
$ri$		Refers to connection from $r$ to subchannel $i$

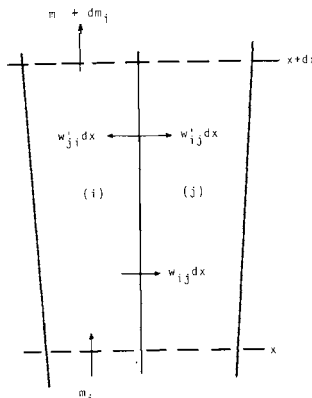
BNWL-1229

APPENDIX A

DERIVATION OF EQUATIONS

APPENDIX ADERIVATION OF EQUATIONS

The equations of continuity, energy and momentum are derived here by applying the conservation equations to a segment of Subchannel (i) which is connected to another Subchannel (j) .

Continuity Equation

A mass balance on Subchannel (i) gives

$$m_i + w'_{ji} dx = m_i + dm_i + w_{1j} dx + w'_{ij} dx \quad (A-1)$$

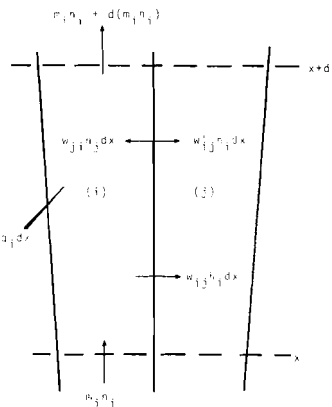
Since by assumption, the turbulent crossflow causes no net flow change ( $w'_{ji} = w'_{ij}$ ), the continuity equation reduces to

$$\frac{dm_i}{dx} = -w_{ij}. \quad (A-2)$$

If the diversion crossflow from (i) to (j) is chosen to be positive, then, by considering all such adjacent subchannels, the continuity equation becomes

$$\frac{dm_i}{dx} = - \sum_{j=1}^N w_{ij} \quad i = 1, 2, \dots, N. \quad (A-3)$$

### Energy Equation



An energy balance on Subchannel (i) gives

$$m_i h_i + w'_{ij} h_j dx + \bar{q}_i^+ dx = w_{ij}^+ h_i dx + w'_{ij} h_i dx + m_i h_i + d(m_i h_i). \quad (A-4)$$

Since, by assumption,  $w_{ij}^+ = w_{ji}^+$ , this reduces to

$$m_i \frac{dh_i}{dx} + h_i \frac{dm_i}{dx} = \bar{q}_i^+ + w_{ij}^+ (h_j - h_i) - w_{ij} h_i. \quad (A-5)$$

This equation applies when the diversion crossflow is from  $i$  to  $j$ . To account for the uncertainty of the enthalpy which is carried through the gap, this equation may be written as

$$m_i \frac{dh_i}{dx} + h_i \frac{dm_i}{dx} = \bar{q}_i^+ + w_{ij}^+ (h_j - h_i) - w_{ij} h^* \quad (A-6)$$

where  $h^*$  is the effective enthalpy that is carried through the gap by the diversion crossflow. If the subchannel enthalpy is uniform,  $h^*$  is defined as

$$h^* = \begin{cases} h_i; & \text{if } w_{ij} > 0 \\ h_j; & \text{if } w_{ij} < 0 \end{cases} \quad (A-7)$$

The **heat** transfer term  $\bar{q}_i^T$  may be divided into two terms. The first is the heat transfer rate from the fuel surface  $q_i'$ , and the second is heat conduction between adjacent subchannels. The heat conduction is assumed to be proportional to the subchannel temperature difference and the constant of proportionality as assumed to be a function of the subchannel geometry and fluid properties.

By considering the heat conduction term and all such adjacent subchannels, the energy equation may be written as

$$m_i \frac{dh_i}{dx} = q_i' + \sum_{j=1}^N (h_i - h_j) w_{ij}^* - \sum_{j=1}^N (t_i - t_j) c_{ij} + \sum_{j=1}^N (h_i - h^*) w_{ij} \quad (A-8)$$

where  $t$  is limited to the saturation temperature during boiling,

#### Axial Momentum Equation

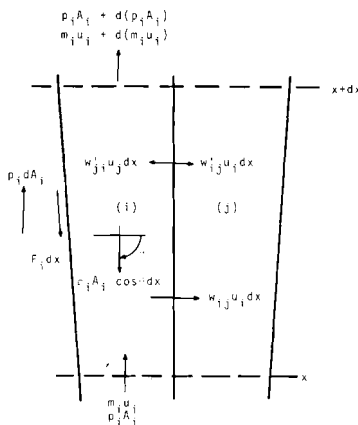
The derivation of the momentum equation is a little more complex than the continuity and energy equations; however, the same technique applies. For a one-dimensional analysis, the momentum in a two-phase flow stream can be defined as

$$\frac{AG^2 v^*}{g_c} = \frac{m^2}{A} \frac{Av^*}{g_c} - \frac{mu}{g_c} \quad (A-9)$$

where **the** momentum velocity is

$$u = \frac{mv^*}{A} \quad (A-10)$$

The effective specific volume term is that used by Meyer<sup>(7)</sup> in his development of two-phase flow equations,



By equating forces acting on Subchannel (i) in the **x** direction to the change in **momentum**, the axial momentum equation is

$$\begin{aligned}
 g_c (A_i p_i - F_i dx - A_i p_i - d(A_i p_i) + p_i dA_i - A_i \rho_i \cos \theta dx) = \\
 + w_{ij} u_i dx + w_{ij}^! u_i dx + m_i u_i + d(m_i u_i) - m_i u_i - w_{ji}^! u_j dx
 \end{aligned} \tag{A-11}$$

By using Equation (A-3) and  $w_{ij}^! = w_{ji}^!$ , this reduces to

$$\begin{aligned}
 \frac{dp_i}{dx} = -\frac{F_i}{A_i} - \rho_i \cos \theta - \frac{w_{ij}^!}{A_i g_c} (u_i - u_j) \\
 - \frac{2u_i}{A_i g_c} \frac{dm_i}{dx} - \frac{u_i w_{ij}}{A_i g_c} - \left(\frac{m_i}{A_i}\right)^2 \frac{A_i}{g_c} \frac{d(v_i^!/A_i)}{dx}.
 \end{aligned} \tag{A-12}$$

As in the derivation of the energy equation, this applies when the diversion crossflow is from i to j. To account for the uncertainty of the axial velocity which is carried through the gap, this equation may be written as

$$\frac{dp_i}{dx} = -\frac{F_i}{A_i} - \rho_i \cos\theta - f_T \frac{w_{ij}^i}{A_i g_c} (u_i - u_j) - \frac{2u_i}{A_i g_c} \frac{dm_i}{dx} - \frac{u^* w_{ij}}{A_i g_c} - \left(\frac{m_i}{A_i}\right)^2 \frac{A_i}{g_c} \frac{d(v_i^i/A_i)}{dx} \quad (A-13)$$

where  $u^*$  is the effective axial velocity that is carried through the gap by the diversion crossflow. The factor  $f_T$  is used to account for an imperfect analogy between the turbulent transport of enthalpy and momentum. If the velocity is uniform in the subchannels,  $u^*$  is defined by

$$u^* = \begin{cases} u_i; & \text{if } w_{ij} \geq 0 \\ u_j; & \text{if } w_{ij} < 0 \end{cases} \quad (A-14)$$

The flow resistance force in a subchannel is assumed to consist of a wall friction term plus an additional drag term which may account for spacing devices or other types of flow blockage. This is given by the equation

$$\frac{F_i}{A_i} = \frac{1}{g_c} \left(\frac{m_i}{A_i}\right)^2 \left[ \frac{v_i f_i \phi_i}{2D_i} + \frac{K_i v_i^i}{2} \right] \quad (A-15)$$

where  $K_i$  is the drag coefficient<sup>8</sup> defined in terms of the unperturbed subchannel velocity,

By substituting Equation (A-15) into Equation (A-13) and by considering all subchannels adjacent to Subchannel (i), the axial momentum equation becomes

$$\begin{aligned} \frac{dp_i}{dx} &= -\frac{1}{g_c} \left(\frac{m_i}{A_i}\right)^2 \left[ \frac{v_i f_i \phi_i}{2D_i} + \frac{K_i v_i^i}{2} + A_i \frac{d(v_i^i/A_i)}{dx} \right] \\ &- \rho_i \cos\theta - \frac{1}{g_c A_i} \sum_{j=1}^N (u_i - u_j) f_T w_{ij}^i \\ &+ \frac{1}{g_c A_i} \sum_{j=1}^N (2u_i - u^*) w_{ij} \\ & \quad i = 1, 2, \dots, N. \end{aligned} \quad (A-16)$$

---

erse Momentum Equation

By neglecting the transverse spatial acceleration, the transverse momentum equation may be written as

$$C_{ij} |w_{ij}| w_{ij} = p_i - p_j \quad (A-17)$$

where  $C_{ij}$  is the transverse crossflow resistance factor.

BNWL-1229

APPENDIX B

GENERALIZED FORM OF THE EQUATIONS

APPENDIX BGENERALIZED FORM OF THE EQUATIONS

This Appendix presents a matrix representation of the mathematical **model's** equations. To set up this notation, it is necessary to introduce some notation to show how the subchannel connections are ordered. The generalized form of the equations will follow directly from the matrix notation,

Matrix Notation

The connections between adjacent subchannels are identified by a matrix  $K$  whose elements are  $k(i,j)$ ; where  $k(i,j) = 0$  if there is no connection and  $k(i,j)$  is assigned a value for each valid connection. The nonzero values of  $k(i,j)$  are assigned in ascending order by considering Subchannel (i) and then assigning connection numbers for each successive connected Subchannel (j) where  $j$  is greater than  $i$ . Therefore, each pair of Subchannels (i) and (j) have a unique connection number. Likewise, each connection number identifies a unique pair of **subchannels**. Let these **subchannels** be denoted by two column vectors  $I$  and  $J$  with elements  $i(k)$  and  $j(k)$ , respectively,

The identification procedure allows the crossflows to be written as a **column** vector with elements

$$w_{k(i,j)} = w_{ij} \quad (B-1)$$

and with a sign convention that for  $w_k > 0$  the flow is from Subchannel (i) to Subchannel (j) where  $i$  is less than  $j$ .

For purposes of notation, let [ ] denote a rectangular matrix that is not necessarily square and let { } denote a column vector,

### Generalized Equations

Let  $[K]$  be a  $(N \times K)$  matrix that performs the summation in Equation (A-3); then, Equation (A-3) has the **form**

$$\left\{ \frac{dm}{dx} \right\} = -[R]\{w\}. \quad (B-2)$$

Similarly, the Energy Equation (A-8) may be written as

$$\begin{aligned} \left\{ m \frac{dh}{dx} \right\} &= \{q'\} - [R] [[h_I] - [h_J]] \{w'\} \\ &\quad - [R] [[t_I] - [t_J]] \{e\} \\ &\quad + [R] [[h_I] - [h^*]] \{w\} \end{aligned} \quad (B-3)$$

where the elements of the  $(K \times K)$  diagonal matrices  $[h_I]$  and  $[h_J]$  are given by  $h_{i(k)}$  and  $h_{j(k)}$ , respectively. The temperature matrixes are defined similarly. The element of the  $(K \times K)$  diagonal matrix  $[h^*]$  are selected from  $[h_I]$  or  $[h_J]$  depending upon the sign of the diversion crossflow.

Equation (B-3) can be reduced to the more compact form

$$\left\{ \frac{dh}{dx} \right\} = \{Q\} - [R][H]\{w'\} - [R][T]\{c\} + [R][I^*]\{w\} \quad (B-4)$$

where

$$\{Q\} = \left\{ \frac{q'}{m} \right\} \quad (B-5)$$

$$[H] = [m_I]^{-1} [[h_I] - [h_J]] \quad (B-6)$$

$$[I^*] = [m_I]^{-1} [[h_I] - [h^*]] \quad (B-7)$$

$$[T] = [m_I]^{-1} [[t_I] - [t_J]] \quad (B-8)$$

In a similar way the Axial Momentum Equation (A-16) may be written in the compact form

$$\left\{ \frac{dp}{dx} \right\} = a - [R][U]\{f_T w'\} + [R][U^*]\{w\} \quad (B-9)$$

where

$$\{a\} = \frac{1}{g_c} \left\{ \left( \frac{m}{A} \right)^2 \left[ \frac{vf\phi}{2D} + \frac{Kv'}{2} + A \frac{d(v/A)}{dx} \right] \right\} + \left\{ \rho \cos \theta \right\} \quad (B-10)$$

$$[U] = \frac{1}{g_c} [A_I]^{-1} [[u_I] - [u_J]] \quad (B-11)$$

$$[U^*] = \frac{1}{g_c} [A_I]^{-1} [[2u_I] - [u^*]] \quad (B-12)$$

The remaining equation is the Transverse Momentum Equation (A-17) which may be written as

$$\{C|w|w\} = [S]\{p\} \quad (B-13)$$

where  $[S]$  is a  $(K \times N)$  matrix that orders the pressure into proper pairs for determining the crossflow for each subchannel connection.

BNWL-1229

APPENDIX C

NUMERICAL STABILITY

APPENDIX CNUMERICAL STABILITY

Numerical stability is concerned with the propagation of errors by the numerical technique as the solution progresses with a finite step size; therefore, a stability analysis is concerned with the possible growth of errors. In other words, will an error at one step tend to increase or decrease as the solution progresses,

The stability of the numerical schemes used in COBRA-II can be investigated by examining the vector equation

$$\frac{dy}{dx} = A y + b \quad (C-1)$$

where **A** is a square matrix of coefficients and **b** is a column vector of coefficients. Since both forward and backward difference approximations are used in COBRA-II, these two approximations to Equation (C-1) will be considered separately,

Forward Difference

By using a forward difference, Equation (C-1) may be written as

$$y(x+\Delta x) = (I + \Delta x A) y(x) + b \quad (C-2)$$

where **I** is the identity matrix. If the solution actually obtained is  $Y(x+\Delta x)$  and it contains an error  $\epsilon(x+\Delta x)$ , it may be written as

$$Y(x+\Delta x) = (I + \Delta x A) Y(x) + b + \epsilon(x+\Delta x) \quad (C-3)$$

If **A** and **b** are assumed constant and the error is bounded by  $|\epsilon(x+\Delta x)| < \delta$ , an equation for determining an upper bound on the propagation of this error is

$$w(x+\Delta x) = (I+\Delta x A) w(x) + \delta \quad (C-4)$$

where  $w = Y - y$ . The solution of this equation may be examined by assuming a solution of the form  $w(x) = C\lambda^n$  where  $n = x/\Delta x$ . This gives

$$C\lambda^{n+1} = (I+\Delta x A)C\lambda^n + \delta \quad (C-5)$$

or, for the homogeneous equation,

$$(I+\Delta x A - \lambda)C\lambda^n = 0. \quad (C-6)$$

Thus the roots of the determinant

$$|I+\Delta x A - \lambda| = 0 \quad (C-7)$$

give the values of  $\lambda$  which are the eigenvalues of  $I+\Delta x A$ . The eigenvector  $C$  can be evaluated in terms of the error bound  $\delta$ . The eigenvalues of  $(I+\Delta x A)$  must all be less than one to prevent the growth of  $C\lambda^n$  and insure stability. If the eigenvalues of  $(I+\Delta x A)$  are of mixed sign, then the largest in absolute value controls the growth of errors. An estimate of the maximum eigenvalue can be obtained by taking norms of Equation (C-6). The result is

$$|\lambda|_{\max} < 1 + \Delta x \|A\|. \quad (C-8)$$

This bound does not indicate when stability occurs, but it does indicate how bad instability can be. If  $\Delta x \|A\|$  is small as compared to unity, then the error growth can not be very fast.

The forward difference approximation is only used for the energy equation in COBRA-11. For this equation, the value of  $\|A\|$  is rather small,

This can be seen by using the infinity norm (maximum-row-sum)

$$\|A\|_{\infty} = \max_i \sum_j |a_{ij}| \quad (C-9)$$

where  $a_{ij}$  are multiples of  $|(w_{ij} - w_{ij}^*)/m_i|$ . For most cases, these are significantly less than one. Also, since there are only a few such quantities for even large problems and  $\Delta x \ll 1$ ,  $|\lambda|_{\max}$  is only a little greater than one. It could actually be less than one. Thus the error growth in the solution of the Energy Equation should not be excessive,

The reason a forward difference is not suitable for the Momentum Equation is easily seen in the above criterion. Note that for a forward difference in Equation (7),  $(I + \Delta x A)$  is equivalent to  $(I + \Delta x (C|w|)^{-1} SRU^*)$  which has very large eigenvalues. Since the value of  $C^{-1}$  is very large as compared to any reasonable  $\Delta x$ , the forward difference is not suitable for solving the momentum equations,

### Backward Difference

By using a backward difference, Equation (C-1) may be approximated by

$$y(x + \Delta w) = (I - \Delta x A)^{-1} y(x) + (I - \Delta x A)^{-1} b \quad (C-10)$$

and the error equation may be written as

$$w(x + \Delta x) = (I - \Delta x A)^{-1} w(x) + \delta \quad (C-11)$$

as in the case of the forward difference a stable solution is obtained if the eigenvalues of  $(I - \Delta x A)^{-1}$  are less than unity. To satisfy this, it is necessary that the eigenvalues of  $(I - \Delta x A)$  be greater than unity. Furthermore, since the condition number is given by  $\text{Cond } (I - \Delta x A) = \|(I - \Delta x A)\| \|(I - \Delta x A)^{-1}\| > 1$ , it is necessary that  $\|(I - \Delta x A)\| = \text{Cond } (I - \Delta x A)$ . Since the condition number can be quite large for a linear system, the eigenvalues of  $(I - \Delta x A)$  may have

to be quite large to insure a stable solution. This can be achieved by selecting a sufficiently large  $\Delta x$ . Unfortunately, there is no easy way to select the minimum allowable  $\Delta x$  because the condition number is not readily available during computation,

A backward difference is used to solve Equation(7). In this case the matrix  $(I - \Delta x A)$  is equivalent to  $(I - \Delta x (C|w|)^{-1} SRU^*)$ . For most rod bundles,  $C^{-1}$  is large; therefore, if  $\Delta x$  is large enough, stable solutions can be obtained,

As an example of what is required to insure stability, consider the case of two subchannels. In this case, the eigenvalue of the inverse is simply

$$\lambda = \frac{1}{1 - \frac{\Delta x SRU^*}{C|w|}}. \quad (C-12)$$

For  $\Delta x = 2 C|w|/SRU^*$  the solution is stable. As  $\Delta x$  approaches  $C|w|/(SRU^*)$  the errors grow and when  $\Delta x = C|w|/(SRU^*)$ , the solution blows up. For  $\Delta x < C|w|/(SRU^*)$  errors grow from flow reversals which are not physically possible,

COBRA-II contains two rather simple checks that test for numerical instability. As in Equation(C-12) the diagonal elements of  $I - \Delta x (C|w|)^{-1} SRU^*$  are checked for sign. If the diagonal elements are positive, the flow solutions will blow up. The second test checks to determine if

$$\| I - \Delta x (C|w|)^{-1} SRU^* \|_{\infty} < K$$

where K is a positive constant. If this test is true then the solution is unstable. Since the constant K is not known, it is set equal to its lower bound  $K = 1.0$  in the present writing of COBRA-II. It should be realized that this test only checks for instability. If the constant K is not large enough, instability could also occur outside this bound. To check for this possibility,

it is suggested that the user of COBRA-II run several calculations at different values of  $\Delta x$ . If errors grow for decreasing  $\Delta x$  then  $\Delta x$  is not large enough. If the errors decrease, then  $\Delta x$  is large enough to insure stability. This type of check is not required for all problems, but it is suggested that a sample problem be examined from a set of similar problems. It should also be noted that an error may grow locally and then diminish. This can be caused by the changing value of  $(C|w|)^{-1}$ . Present experience with COBRA-II indicates that  $\Delta x$  on the order of one inch easily satisfies the stability criteria for most rod bundles. This is usually small enough to get good numerical solutions,

BNWL-1229

APPENDIX D

COMPUTER PROGRAM CORRELATIONS

APPENDIX DCOMPUTER PROGRAM CORRELATIONS

To carry out a solution, empirical and semiempirical correlations must be selected for input to the computer program. The following correlations are an example of what is available,

Friction Factor

The friction factor correlation is assumed to be of the form<sup>(8)</sup>

$$f_i = a(R_{e_i})^b + c \quad (D-1)$$

where  $a$ ,  $b$ , and  $c$  are specified **constants** that depend upon the subchannel roughness and geometry. Since these constants can be influenced by different subchannel roughnesses and the pitch-to-diameter ratio,<sup>(9)</sup> the program can accept up to four sets of constants that correspond to four subchannel types which may be assigned to the **subchannels** of the bundle. For example, **subchannels** next to a flow housing may be given a different friction factor from those **subchannels** within the bundle,

The friction factor is also corrected for wall viscosity by using the relationship<sup>(9)</sup>

$$\frac{f}{f_{iso}} = \left( \frac{\mu_{wall}}{\mu_{bulk}} \right)^{0.6} \quad (D-2)$$

where  $\mu_{wall}$  is evaluated at the wall temperature which is calculated from

$$t_{wall} = t_{bulk} + \frac{q}{h} \quad (D-3)$$

The heat transfer coefficient is calculated from

$$\frac{hD}{\mu} = 0.023 \left( \frac{GD}{\mu} \right)^{0.8} \left( \frac{C_p}{k} \right)^{0.4} \quad (D-4)$$

where bulk fluid properties are used,

Two-Phase Friction Multiplier

Several correlations are available for the two-phase friction multiplier. Three are presently included in the program.

Homogeneous Model

$$\phi = 1.0 \quad X < 0,$$

$$\phi = \frac{\rho_f}{\rho} \quad X > 0. \quad (D-5)$$

Armand<sup>(10)</sup>

$$\phi = 1.0 \quad \alpha \leq 0$$

$$\phi = \frac{(1-X)^2}{(1-\alpha)^{1.42}} \quad 0.39 < (1-\alpha) \leq 1.0$$

$$\phi = 0.478 \frac{(1-X)^2}{(1-\alpha)^{2.2}} \quad 0.1 < (1-\alpha) \leq 0.39$$

$$\phi = 1.730 \frac{(1-X)^2}{(1-\alpha)^{1.64}} \quad 0. < (1-\alpha) \leq 0.1 \quad (D-6)$$

Polynomial Function

$$\phi = 1.0 \quad X < 0$$

$$\phi = a_0 + a_1 X + a_2 X^2 + \dots a_n X^n \quad X > 0 \quad (D-7)$$

where the coefficients are supplied as input,

Spacer Loss Coefficient

The pressure drop from spacers is lumped into an effective loss coefficient which may be defined<sup>(9)</sup> in terms of all liquid flow as

$$\Delta P = \frac{K}{2g_s} \left( \frac{a}{\Delta x} \right)^2 \quad (D-8)$$

For two-phase flow the same coefficient is used but it is modified by the two-phase specific volume for momentum. This pressure drop loss coefficient is converted to a pressure gradient loss coefficient at the location of the spacer by dividing by the calculation increment  $\Delta x$ ; therefore,

$$K_i = \frac{K}{\Delta x} . \quad (D-9)$$

This is the coefficient used in Equation (A-15).

#### Void Fraction

Four ways of specifying void fraction are presently included in the program:

##### Homogeneous Model

$$\alpha = 0. \quad X \leq 0. \quad (D-10)$$

$$\alpha = \frac{Xv_g}{(1-X)v_f + Xv_g} \quad X > 0.$$

##### Slip Model

$$\alpha = 0. \quad X \leq 0. \quad (D-11)$$

$$\alpha = \frac{Xv_g}{(1-X)v_f + Xv_g} \quad X > 0.$$

where  $\gamma$  is a specified slip ratio.

##### Modified Armand<sup>(11)</sup>

$$\alpha = 0. \quad X \leq 0. \quad (D-12)$$

$$\alpha = \frac{(0.833+0.167X)Xv_g}{(1-X)v_f + Xv_g} \quad X > 0.$$

Polynomial Function

$$\alpha = 0. \quad X < 0. \quad (D-13)$$

$$\alpha = a_0 + a_1 X + a_2 X^2 + \dots a_n X_n \quad X > 0.$$

Subcooled Void Fraction

Two options are presently included. Subcooled void formation may be ignored or it may be included by using Levy's subcooled void model. Levy's model calculates the true quality in terms of the equilibrium quality in terms of the quality at which bubble departure starts. It is given by

$$X = 0. \quad X_e < X_d \quad (D-14)$$

$$X = X_e - X_d \exp\left(\frac{X_e}{X_d} - 1\right) \quad X_e/X_d < 1$$

where  $X_e$  is the equilibrium quality and

$$X_d = -\frac{C_p \Delta t}{h_{fg}} \quad (D-15)$$

$$\Delta t = \frac{q'}{P_h h} - Q P_r Y_B \quad 0 < Y_B \leq 5$$

$$\Delta t = \frac{q'}{P_h h} - 5Q(P_r + \log(1 + P_r(2Y_B - 1))) \quad 5 < Y_B \leq 30$$

$$\Delta t = \frac{q'}{P_h h} - 5Q(P_r + \log(1 + 5P_r) + \frac{1}{2} \log(\frac{Y_B}{30})) \quad 30 < Y_B \quad (D-16)$$

$$Q = \frac{q'}{P_h v} C_p \sqrt{\tau_w g_c v} \quad (D-17)$$

$$\tau_w = \frac{fv}{8g_c} \left( \frac{m}{A} \right)^2 \quad (D-18)$$

$$Y_B = \frac{0.015}{\mu} \sqrt{\frac{\sigma g_c D}{v}} \quad (D-19)$$

The heat transfer coefficient  $h$  is calculated from Equation (D-4).

#### Single-Phase Turbulent Mixing

Several forms of equations for specifying the turbulent crossflow are included. Although they specify the turbulent mixing parameter  $\beta$ , the final result is the turbulent crossflow rate given by

$$w_{ij} = \beta_{ij} s_{ij} \frac{m_i + m_j}{A_i + A_j} \quad (D-20)$$

The presently available forms in COBRA-II for calculating  $\beta$  include:

$$\beta_{ij} = a \quad (D-21)$$

$$\beta_{ij} = a Re^b \quad (D-22)$$

$$\beta_{ij} = \frac{4}{s_{ij}} \frac{A_i + A_j}{P_{w_i} + P_{w_j}} a Re^b \quad (D-23)$$

$$\beta_{ij} = \frac{4}{z_{ij}} \frac{A_i + A_j}{P_{w_i} + P_{w_j}} a Re^b \quad (D-24)$$

$$\text{where } Re = \frac{8(m_i + m_j)}{(P_{w_i} + P_{w_j})(\mu_i + \mu_j)} \quad (D-25)$$

and  $a$  and  $b$  are input constants. Since a definitive mixing correlation does not exist and other forms are available,<sup>(13)</sup> the user should set up correlations of his choice,

Also included in the subcooled mixing is the **thermal** conduction. When it is included, the conduction coefficient is given by

$$c_{ij} = \left( \frac{k_i + k_j}{2} \right) \frac{s_{ij}}{z_{ij}} K_g \quad (D-26)$$

where  $K_g$  is a geometric correction factor. Note that the distance  $z_{ij}$  is used in both Equations (D-24) and (D-26). This is the centroid-to-centroid distance between subchannels. Care should be taken to select this value for its intended use. For example,  $z_{ij}$  could be selected as the effective mixing as identified by Todreas and Rogers. (13)

### Two-Phase Turbulent Mixing

Complete information concerning mixing during boiling is not available. It is known, however, that mixing is strongly dependent on quality; therefore, COBRA-II is set up to accept  $\beta$  as tabular function of quality. When the quality of two adjacent subchannels is different, the calculations use a quality calculated from the mean mixed enthalpy of the two subchannels,

### Transverse Crossflow Resistance

To obtain an **estimate** of the transverse crossflow resistance, a simple friction model is used. If the gap is assumed to be a slot of spacing  $s$  and a wide, the resistance coefficient is

$$C_{ij} = \frac{f\ell}{4g_c s^3 \rho_i} \quad (D-27)$$

where  $f$  is a selected friction factor. The product  $f\ell$  is an arbitrary constant that is input to the problem. The **density**  $\rho_i$  is taken in lieu of a two-phase friction multiplier for the transverse two-phase flow,

### Power Distribution

The heat input per unit length of channel is the **sum** of all such inputs from fuel rods adjacent to the subchannel. The **heat transfer** ( $q'_ri$ ) from a rod ( $r$ ) to a subchannel ( $i$ ) is given by

$$q'_{ri} = \bar{q}' D_r f_c f_R f_A (x/L) \quad (D-28)$$

where  $\int_0^1 f_A(x/L) d(x/L) = 1.$  (D-29)

The sum of the heat inputs from rods adjacent to Subchannel (i) is the total heat input per unit length ( $q_i$ ).

BNWL-1229

APPENDIX E

SAMPLE PROBLEM

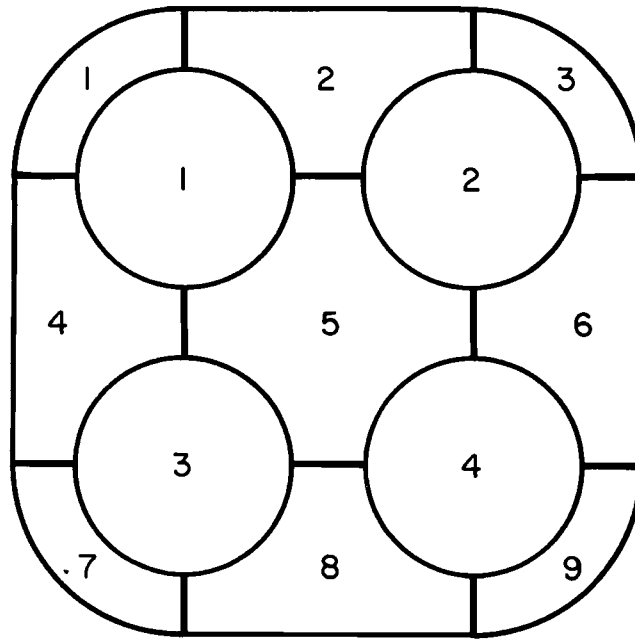
APPENDIX EDIGITAL COMPUTER PROGRAM SAMPLE PROBLEM

A 4-rod bundle is used for the sample problem to show the input for COBRA-11. The subchannel and fuel rod numbering scheme is shown in the sketch and the nominal dimensions of the three types of subchannels are given in the table. The axial power distribution is assumed to be uniform. The radial power distribution is skewed with relative powers of 1.2, 1.0, 1.0 and 0.8 in Rods 1, 2, 3 and 4, respectively. The operating conditions are: 1000 psia,  $0.4 \times 10^6$  Btu/hr ft<sup>2</sup> heat flux,  $1.0 \times 10^6$  lb/hr-ft<sup>2</sup> mass velocity and 500 Btu/lb inlet enthalpy.

Several of the new features of COBRA are illustrated by the input. The outer wall subchannels are designated as Type 1 and are given a higher friction factor than the interior subchannel designed as Type 2. A blockage is assumed to occur in Subchannel 1 that reduces the flow area and gap spacing at  $x/L = 0.2$ . Two types of spacers are considered. Type 1 simulates the inlet and exit pressure losses and Type 2 simulates losses of 3 grid spacers. These spacers have flow diverters that divert flow into Subchannel 5 from Subchannels 2 and 8. The loss coefficients of the diverters are also assumed to be greater. The mixing parameter  $\beta$  is assumed to be constant for single-phase flow and a function of quality for two-phase flow. Output options are selected to print the exit summary, crossflows and complete answers for Subchannels 1, 4 and 5,

Subchannels	SUBCHANNEL DIMENSIONS <sup>(a)</sup>		
	Area (in. <sup>2</sup> )	Wetted Perimeter (in.)	Heater Perimeter (in.)
1,3,7,9	0.0783	1.116	0.4476
2,4,6,8	0.1824	1.633	0.8954
5	0.2894	1.791	1.791

(a) Rod-to-rod spacing 0.168 in.; Rod-to-wall spacing 0.135 in,  
Rod diameter 0.570 in.; Length 72.0 in,



Page E-3 contains a complete listing of the input data for the **sample** problem. Pages E-4 through E-8 contain the computer input for the sample problem.

1 1 30 SAMPLE PROBLEM FOR COBRA TO ILLUSTRATE INPUT.

50.2814.0	0.017274	8.5140	250.2	1174.1	0.491	0.3959	0.003012
100.3274.8	0.017740	4.4310	298.5	1187.2	0.410	0.3936	0.002606
150.3584.4	0.01809	3.0139	330.6	1194.1	0.369	0.3893	0.002350
200.3814.8	0.01839	2.2873	355.5	1198.3	0.345	0.3852	0.00209
250.4014.0	0.01865	1.8432	376.1	1201.1	0.326	0.3806	0.00193
300.4174.4	0.01889	1.5427	394.0	1202.9	0.313	0.3760	0.00180
350.4314.7	0.01912	1.3255	409.8	1204.0	0.301	0.3718	0.00168
400.4444.6	0.01934	1.1610	424.2	1204.6	0.290	0.3682	0.00158
440.4544.0	0.01950	1.0554	434.8	1204.8	0.283	0.3658	0.00150
480.4624.8	0.01967	0.9668	444.7	1204.8	0.278	0.3631	0.00144
520.4714.1	0.01982	0.89137	454.2	1204.5	0.273	0.3604	0.00138
560.4784.8	0.01988	0.82637	463.1	1204.2	0.269	0.3580	0.00132
600.4864.2	0.02013	0.76975	471.7	1203.7	0.264	0.3550	0.00127
640.4934.2	0.02028	0.71995	479.9	1203.0	0.260	0.3552	0.00122
680.4994.9	0.02043	0.67581	487.7	1202.3	0.255	0.3494	0.00117
720.5064.2	0.02058	0.63639	495.4	1201.4	0.252	0.3462	0.00113
760.5124.3	0.02072	0.60097	502.7	1200.4	0.248	0.3435	0.00108
800.5184.2	0.02087	0.56896	509.8	1199.4	0.245	0.3405	0.00104
840.5234.9	0.02101	0.53988	516.7	1198.2	0.242	0.3377	0.00100
880.5294.3	0.02116	0.51333	523.4	1197.0	0.240	0.3350	0.00096
920.5344.6	0.02130	0.48901	530.0	1195.7	0.237	0.3325	0.00092
960.5394.7	0.02145	0.46662	536.3	1194.4	0.234	0.3299	0.00089
1000.5444.6	0.02159	0.44595	542.4	1192.9	0.232	0.3275	0.00086
1040.5494.4	0.02174	0.42681	548.6	1191.4	0.229	0.3243	0.00082
1080.5544.0	0.02188	0.40902	554.6	1189.9	0.227	0.3224	0.00079
1120.5584.5	0.02203	0.39244	560.5	1188.2	0.225	0.3198	0.00076
1160.5624.9	0.02217	0.37695	566.2	1186.6	0.223	0.3174	0.00073
1200.5674.2	0.02232	0.36245	571.9	1184.8	0.221	0.3140	0.00070
1240.5714.4	0.02247	0.34884	577.4	1183.0	0.219	0.3113	0.00068
1280.5754.4	0.02262	0.33603	582.9	1181.2	0.217	0.3086	0.00065
2 1 0 0							
316 -.25	0. .400	-.25	0.				
3 2							
0. 1. 1. 1.							
4 9 9							
2 1.07831.116.4476		2 .135		4 .135			
2 2.18241.633.8954		3 .135		5 .168			
2 3.07831.116.4476		6 .135					
2 4.18241.633.8954		5 .168		7 .135			
1 5.28541.7911.791		6 .168		8 .168			
2 6.18241.633.8954		9 .135					
2 7.07831.116.4476		8 .135					
2 8.18241.633.8954		9 .135					
2 9.07831.116.4476							
5 1 5							
0. .1 .2 .3 1.							
1 1. 1. 5 1. 1.							
6 2 5							
0. .1 .2 .3 1.							
1 2							
1. 1. 5 1. 1.							
1. 4							
1. 1. 5 1. 1.							
7 2 5 2							
0.0001 1 .25 2 .5 2 .75 2 1. 1							
1 .3 0. 0							
2 .3 0. 0							
3 .3 0. 0							
4 .3 0. 0							
5 .3 0. 0							
6 .3 0. 0							
7 .3 0. 0							
8 .3 0. 0							
9 .3 0. 0							
1 .2 0. 0							
2 .2 0. 0							
3 .2 0. 0							
4 .2 0. 0							
5 .2 0. 0							
6 .2 0. 0							
7 .2 0. 0							
8 .4 0. 3 5							
9 .2 0. 0							
8 4 4							
1 .570 1.2 1 .25 2 .25 4 .25 5 .25							
2 .570 1.0 2 .25 3 .25 5 .25 6 .25							
3 .570 1.0 4 .25 5 .25 7 .25 8 .25							
4 .570 .8 5 .25 6 .25 8 .25 9 .25							
9							
.001 1. 72. 0. 25 6							
.01 0. 0. 05 .06 .1 .06 .25 .02 .6 .01							
11 0 0 0							
1000. 500. 1. .4							
12 1 3							
1 4 5							
0							
0							

## INPUT FOR CASE 1 SAMPLE PROBLEM FOR COBRA TO ILLUSTRATE INPUT.

## FLUID PROPERTY TABLE

P	V	T	Y0	HF	HG	WISC.	KF	SIGMA
20.0	281.00	.01727	8.51+00	.250+20	1174.10	.49100	.39500	.00301
100.0	327.80	.01774	4.45100	.298+50	1187.20	.41000	.39300	.00261
150.0	456.40	.01805	3.01300	.350+80	1194.10	.36900	.38300	.00235
200.0	581.80	.01835	2.28700	.355+50	1198.30	.34500	.38520	.00209
250.0	401.00	.01865	1.64300	.376+10	1201.10	.32600	.38060	.00193
300.0	417.40	.01895	1.54270	.394+00	1202.90	.31300	.37600	.00180
350.0	431.70	.01912	1.32550	.409+80	1204.00	.30100	.37180	.00168
400.0	444.00	.01930	1.16100	.424+20	1204.60	.29000	.36820	.00158
450.0	454.00	.01950	1.05500	.434+80	1204.80	.28300	.36580	.00150
480.0	462.80	.01967	.90000	.444+70	1204.80	.27800	.36310	.00144
520.0	471.10	.01982	.89100	.454+00	1204.50	.27300	.36040	.00138
560.0	476.80	.01987	.82637	.463+10	1204.20	.26900	.35800	.00132
600.0	486.00	.02013	.76975	.471+70	1203.70	.26400	.35500	.00127
640.0	495.20	.02026	.71995	.479+90	1203.00	.26000	.35520	.00122
680.0	499.90	.02043	.67561	.487+70	1202.50	.25500	.34940	.00117
720.0	506.20	.02056	.65039	.495+40	1201.40	.25200	.34620	.00113
760.0	512.30	.02072	.60997	.502+70	1200.40	.24800	.34350	.00108
800.0	518.20	.02087	.56089	.509+80	1199.40	.24500	.34050	.00104
840.0	525.50	.02101	.53548	.516+70	1198.20	.24200	.33710	.00100
880.0	529.30	.02116	.51533	.523+40	1197.00	.24000	.33500	.00096
920.0	534.60	.02130	.48901	.530+00	1195.70	.23700	.33250	.00092
960.0	539.70	.02145	.46062	.536+30	1194.40	.23400	.32990	.00089
1000.0	544.60	.02159	.44556	.542+40	1192.50	.23200	.32750	.00086
1040.0	549.40	.02174	.42081	.548+00	1191.40	.22900	.32440	.00082
1080.0	554.00	.02188	.40562	.554+00	1189.50	.22700	.32240	.00079
1120.0	558.50	.02203	.39244	.560+50	1188.20	.22500	.31960	.00076
1160.0	562.90	.02217	.37695	.566+20	1186.60	.22300	.31740	.00073
1200.0	567.20	.02232	.36495	.571+90	1184.60	.22100	.31400	.00070
1240.0	571.40	.02247	.34864	.577+40	1183.00	.21900	.31130	.00068
1280.0	575.40	.02260	.33603	.582+40	1181.20	.21700	.30860	.00065

## FRICTION FACTOR CORRELATION

CHANNEL TYPE 1 FRICT = .310\*RE\*\*(-.250) + .0000  
 CHANNEL TYPE 2 FRICT = .400\*RE\*\*(-.250) + .0000

## TWO-PHASE FLOW CORRELATIONS

LEVY SUBCOOLED VOID CORRELATION  
 HOMOGENEOUS BULK VOID MODEL  
 HOMOGENEOUS MULLER FRICTION MULTIPLIER

## HEAT FLUX DISTRIBUTION

X/L RELATIVE FLUX  
 .000 1.000  
 1.000 1.000

## SUBCHANNEL INPUT DATA

CHANNEL NO.	TYPE	AREA (SG=1) 1	NETTLETT	HEATED	HYDRAULIC DIAMETER (IN)	(ADJACENT CHANNEL NO., SPACING, CNTRD10 DISTANCE)
1	2	.078300	1.116000	.447600	.280645	( 2, .135+-0.000)( 4, .135+-0.000)( -0, .000+-0.000)( -0, .000+-0.000)
2	2	.182400	1.035000	.489540	.446765	( 3, .135+-0.000)( 5, .135+-0.000)( -0, .000+-0.000)( -0, .000+-0.000)
3	2	.078300	1.116000	.447600	.280645	( 4, .135+-0.000)( 6, .135+-0.000)( -0, .000+-0.000)( -0, .000+-0.000)
4	2	.182400	1.035000	.489540	.446765	( 5, .135+-0.000)( 7, .135+-0.000)( -0, .000+-0.000)( -0, .000+-0.000)
5	1	.269400	1.741000	.1791000	.046543	( 6, .168+-0.000)( 8, .168+-0.000)( -0, .000+-0.000)( -0, .000+-0.000)
6	2	.182400	1.035000	.295400	.446765	( 9, .135+-0.000)( -0, .000+-0.000)( -0, .000+-0.000)( -0, .000+-0.000)
7	2	.078300	1.116000	.447600	.280645	( 8, .135+-0.000)( -0, .000+-0.000)( -0, .000+-0.000)( -0, .000+-0.000)
8	2	.182400	1.035000	.295400	.446765	( 9, .135+-0.000)( -0, .000+-0.000)( -0, .000+-0.000)( -0, .000+-0.000)
9	2	.078300	1.116000	.447600	.280645	( -0, .000+-0.000)( -0, .000+-0.000)( -0, .000+-0.000)( -0, .000+-0.000)

## X/L AREA VARIATION FACTORS FOR SUBCHANNEL (1)

( 1 )  
 .000 1.000  
 .100 1.000  
 .200 .500  
 .300 1.000  
 1.000 1.000

## X/L GAP SPACING VARIATION FACTORS FOR ADJACENT SUBCHANNELS (1,2)

( 1, 2 ) ( 1, 4 )  
 .000 1.000  
 .100 1.000  
 .200 .500  
 .300 1.000 1.000  
 1.000 1.000 1.000

## SPACER DATA

SPACER TYPE NO. 1 2 2 2 1  
 LOCATION (X/L) .000 .250 .500 .750 1.000

SPACER TYPE NO.	CHANNEL	DRAG COEFF.	FRACTION OF FLUX DIVERTED	CHANNEL DIVERTED TO
1		.5000	.0000	0
2		.5000	.0000	0
3		.5000	.0000	0
4		.5000	.0000	0
5		.5000	.0000	0
6		.5000	.0000	0
7		.5000	.0000	0
8		.5000	.0000	0
9		.5000	.0000	0

SPACER TYPE 2

CHANNEL NO.	DIAM. COEFF.	FRACTION OF FLOW DIVERTED	CHANNEL DIVERTED TO
1	.2000	.0000	0
2	.4000	.3000	5
5	.2000	.0000	0
4	.2000	.0000	0
5	.2000	.0000	0
6	.2000	.0000	0
7	.2000	.0000	0
8	.4000	.3000	5
3	.2000	.0000	0

ROD INPUT DATA

ROD NO.	DIAMETER (IN.)	RADIAL POWER FACTOR	FRACTION OF POWER TO ADJACENT CHANNELS (ADJ. CHANNEL NO.)
1	.5700	1.2000	.2500( 1) .2500( 2) .2500( 51) -.0000(-0) -.0000(-0)
2	.5700	1.0000	.2500( 2) .2500( 31) .2500( 5) -.0000(-0) -.0000(-0)
3	.5700	1.0000	.2500( 4) .2500( 51) .2500( 71) .2500( 8) -.0000(-0) -.0000(-0)
4	.5700	.8000	.2500( 5) .2500( 61) .2500( 6) .2500( 9) -.0000(-0) -.0000(-0)

CALCULATION PARAMETERS

TRANS. FRICITION (FT.)	.0010
MOMENTUM TURBULENT FACTOR	1.0000
CHANNEL LENGTH	72.00 INCHES
CHANNEL ORIENTATION	.0 DEGREES
DIVISION FOR PRINT-OUT	25
CALCULATION SUBDIVISION	6
CALCULATION INCREMENT	.500 INCHES

MIXING CORRELATIONS

SUBCOOLED MIXING, BETA = .0100
CONDUCTION MIXING, GEOMETRY FACTOR = .0000
BOILING MIXING, BETA IS A FUNCTION OF STEAM QUALITY
X BETA(X)
.000 .010000
.050 .060000
.100 .010000
.250 .020000
.500 .010000

OPERATING CONDITIONS

SYSTEM PRESSURE	= 1000.0 PSIA
INLET ENTHALPY	= 500.0 BTU/LB
AVG. MASS VELOCITY	= 1.000 MILLION LB/(HR-SQFT)
INLET TEMPERATURE	= 510.0 DEGREES F
AVG. HEAT FLUX	= .400 MILLION BTU/(HR-SQFT)

INITIAL CHANNEL CONDITIONS

UNIFORM INLET ENTHALPY SPECIFIED
UNIFORM MASS VELOCITY

BUNDLE AVERAGED RESULTS

CASE 1 SAMPLE PROBLEM FOR COBRA TO ILLUSTRATE INPUT.

DISTANCE (IN.)	DELTA-H (PSI)	ENTHALPY (BTU/LB)	TEMP. (DEG-F)	QUALITY (M-LB/HR-FT2)	MASS VEL (M-LB/HR-FT2)	Avg Flux (M-BTU/HR-FT2)	Max Flux (M-BTU/HR-FT2)
3.00	-.177	506.45	515.42	.0057	1.0000	.4000	.4800
6.00	-.301	512.96	520.76	.0093	1.0000	.4000	.4800
9.00	-.428	519.36	526.04	.0137	1.0074	.4000	.4800
12.00	-.557	525.80	531.23	.0184	1.0200	.4000	.4800
15.00	-.687	532.27	536.44	.0233	1.0277	.4000	.4800
18.00	-.820	538.72	541.65	.0287	1.0149	.4000	.4800
21.00	-.954	545.17	544.60	.0342	1.0025	.4000	.4800
24.00	-1.089	551.62	544.60	.0407	1.0000	.4000	.4800
27.00	-1.224	558.07	544.60	.0474	1.0000	.4000	.4800
30.00	-1.343	564.52	544.60	.0552	1.0000	.4000	.4800
33.00	-1.589	570.97	544.60	.0629	1.0000	.4000	.4800
36.00	-1.739	577.42	544.60	.0709	1.0000	.4000	.4800
39.00	-2.001	583.88	544.60	.0789	1.0000	.4000	.4800
42.00	-2.159	590.33	544.60	.0874	1.0000	.4000	.4800
45.00	-2.320	596.78	544.60	.0960	1.0000	.4000	.4800
48.00	-2.484	603.23	544.60	.1047	1.0000	.4000	.4800
51.00	-2.652	609.68	544.60	.1135	1.0000	.4000	.4800
54.00	-2.824	616.14	544.60	.1225	1.0000	.4000	.4800
57.00	-3.155	622.59	544.60	.1314	1.0000	.4000	.4800
60.00	-3.335	629.04	544.60	.1406	1.0000	.4000	.4800
63.00	-3.519	635.49	544.60	.1498	1.0000	.4000	.4800
66.00	-3.707	641.94	544.60	.1591	1.0000	.4000	.4800
69.00	-3.899	648.40	544.60	.1684	1.0000	.4000	.4800
72.00	-4.095	654.85	544.60	.1778	1.0000	.4000	.4800

CHANNEL RESULTS

CASE 1 SAMPLE PROBLEM FOR COBRA TO ILLUSTRATE INPUT.

SUMMARY OF RESULTS, EXIT CONDITIONS

CHANNEL NO.	DELTA-H (PSI)	ENTHALPY (BTU/LB)	DELTA-T (DEG-F)	TEMP. (DEG-F)	DELTA-T (DEG-F)	QUALITY (M-LB/HR-FT2)	MASS VEL (LB/HR)	FLOW (LB/HR)
1	-4.095	603.45	165.45	544.60	34.56	.1861	.9662	.9276
2	-4.095	608.35	158.35	544.60	34.56	.1870	.9706	1229.46
3	-4.095	605.81	155.81	544.60	34.56	.1783	.9278	504.50
4	-4.095	605.16	158.16	544.60	34.56	.1869	.9746	1234.50
5	-4.095	605.56	155.56	544.60	34.56	.1764	1.0813	2173.16
6	-4.095	605.96	149.96	544.60	34.56	.1695	1.0267	1300.54
7	-4.095	606.21	156.21	544.60	34.56	.1807	.9217	501.17
8	-4.095	606.31	150.31	544.60	34.56	.1717	1.0170	1228.21
9	-4.095	606.25	148.65	544.60	34.56	.1655	.9694	527.09
Avg	-4.095	604.85	154.85	544.60	34.56	.1778	1.0000	9251.39

## CHANNEL RESULTS

CASE 1 SAMPLE PROBLEM FOR COBRA TO ILLUSTRATE INPUT.  
CHANNEL 1

DISTANCE (IN.)	DELTA-P (PSI)	ENTHALPHY (BTU/LB)	TEMP. (DEG-F)	QUALITY	MASS VEL (M-LB/HR-FT2)	FLOW (LB/HR)	FLUX (M-BTU/HR-FT2)
.00	.000	500.00	510.04	.0061	1.0000	5.3375	.4801
.500	-.177	506.40	517.00	.0125	.9178	999.07	.4801
1.00	-.301	516.97	524.12	.0204	.8665	471.17	.4801
1.500	-.428	526.14	530.74	.0235	.8875	469.82	.4801
2.000	-.557	533.34	537.31	.0241	1.1812	428.17	.4801
2.500	-.686	542.74	544.60	.0238	1.2047	354.82	.4801
3.000	-.820	550.39	544.60	.0172	.9893	403.44	.4801
3.500	-.924	553.31	544.60	.0187	.9863	513.98	.4801
4.000	-.160	559.17	544.60	.0275	1.0065	567.30	.4801
4.500	-.1299	565.16	544.60	.0366	1.0114	555.39	.4801
5.000	-.1443	571.34	544.60	.0455	1.0188	553.96	.4801
5.500	-.1589	577.69	544.60	.0548	1.0086	548.41	.4801
6.000	-.1739	584.15	544.60	.0643	.9960	541.59	.4801
6.500	-.2001	589.65	544.60	.0729	1.0104	549.41	.4801
7.000	-.2159	596.26	544.60	.0829	.9859	536.11	.4801
7.500	-.2324	602.93	544.60	.0931	.9712	528.08	.4801
8.000	-.2484	609.61	544.60	.1033	.9597	521.83	.4801
8.500	-.2652	616.32	544.60	.1136	.9500	516.58	.4801
9.000	-.2824	623.05	544.60	.1240	.9417	512.03	.4801
9.500	-.3159	626.62	544.60	.1325	.9601	512.05	.4801
10.000	-.3355	635.50	544.60	.1432	.9404	511.35	.4801
10.500	-.3519	642.54	544.60	.1539	.9287	504.98	.4801
11.000	-.3707	649.51	544.60	.1646	.9200	500.26	.4801
11.500	-.3899	656.46	544.60	.1753	.9128	496.32	.4801
12.000	-.4095	663.45	544.60	.1861	.9062	492.76	.4801

## CHANNEL RESULTS

CASE 1 SAMPLE PROBLEM FOR COBRA TO ILLUSTRATE INPUT.  
CHANNEL 4

DISTANCE (IN.)	DELTA-P (PSI)	ENTHALPHY (BTU/LB)	TEMP. (DEG-F)	QUALITY	MASS VEL (M-LB/HR-FT2)	FLOW (LB/HR)	FLUX (M-BTU/HR-FT2)
.00	.000	500.00	510.04	.0054	1.0000	126.67	.4400
.500	-.177	506.61	515.55	.0099	.9808	1242.36	.4400
1.000	-.301	513.45	521.22	.0148	.9707	1249.51	.4400
1.500	-.428	520.40	526.94	.0209	.9579	1213.36	.4400
2.000	-.557	527.60	532.67	.0268	.9648	1222.11	.4400
2.500	-.686	535.70	538.45	.0327	.9768	1237.27	.4400
3.000	-.820	541.76	544.60	.0403	.9507	1204.28	.4400
3.500	-.924	547.90	544.60	.0459	.9457	1177.85	.4400
4.000	-.160	554.83	544.60	.0522	.9338	1182.87	.4400
4.500	-.1299	561.50	544.60	.0592	.9301	1176.13	.4400
5.000	-.1443	568.10	544.60	.0666	.9309	1179.16	.4400
5.500	-.1589	574.65	544.60	.0744	.9337	1126.66	.4400
6.000	-.1739	581.10	544.60	.0823	.9372	1157.14	.4400
6.500	-.2001	588.67	544.60	.0902	.9550	1209.68	.4400
7.000	-.2159	595.26	544.60	.0984	.9539	1208.31	.4400
7.500	-.2324	602.82	544.60	.1067	.9541	1208.53	.4400
8.000	-.2484	609.34	544.60	.1152	.9556	1210.38	.4400
8.500	-.2652	612.80	544.60	.1239	.9576	1212.98	.4400
9.000	-.2824	619.30	544.60	.1327	.9599	1215.87	.4400
9.500	-.3159	625.10	544.60	.1413	.9792	1240.32	.4400
10.000	-.3355	631.70	544.60	.1501	.9764	1236.72	.4400
10.500	-.3519	638.32	544.60	.1591	.9766	1234.54	.4400
11.000	-.3707	644.94	544.60	.1683	.9740	1233.73	.4400
11.500	-.3899	651.50	544.60	.1775	.9741	1233.84	.4400
12.000	-.4095	658.10	544.60	.1869	.9746	1234.50	.4400

## CHANNEL RESULTS

LASE 1 SAMPLE PROBLEM FOR COBRA TO ILLUSTRATE INPUT.  
 CHANNEL 5 I

DISTANCE	DELTA-P	ENTHALPY	TEMP.	QUALITY	MASS VEL	FLOW	FLUX
(IN.)	(PSI)	(BTU/LB)	(DEG-F)		(M-LB/HR-FT2)	(LB/HR)	(M-BTU/HR-FT2)
0.00	0.000	500.00	510.04	.0007	1.0000	2009.72	.3999
3.00	-1.177	507.19	516.03	.0025	1.0513	2112.87	.3999
6.00	-1.301	515.97	521.65	.0054	1.0835	2177.58	.3999
9.00	-1.428	520.55	526.98	.0095	1.0980	2206.68	.3999
12.00	-1.557	526.9-	532.13	.0141	1.1111	2232.94	.3999
15.00	-1.687	533.24	537.22	.0191	1.1215	2253.84	.3999
18.00	-1.800	539.50	542.27	.0251	1.1199	2250.63	.3999
21.00	-1.924	545.36	544.60	.0310	1.1029	2216.54	.3999
24.00	-1.156	551.96	544.60	.0375	1.0986	2207.81	.3999
27.00	-1.299	538.51	544.60	.0445	1.0941	2198.90	.3999
30.00	-1.443	535.01	544.60	.0518	1.0900	2190.69	.3999
33.00	-1.584	571.48	544.60	.0594	1.0870	2184.61	.3999
36.00	-1.739	577.96	544.60	.0674	1.0846	2179.77	.3999
39.00	-2.001	584.20	544.60	.0752	1.0774	2165.36	.3999
42.00	-2.159	590.85	544.60	.0839	1.0773	2165.03	.3999
45.00	-2.320	597.36	544.60	.0927	1.0770	2164.51	.3999
48.00	-2.484	603.84	544.60	.1015	1.0766	2163.60	.3999
51.00	-2.652	610.31	544.60	.1106	1.0763	2163.13	.3999
54.00	-2.824	616.77	544.60	.1197	1.0763	2163.10	.3999
57.00	-3.155	623.02	544.60	.1284	1.0696	2149.62	.3999
60.00	-3.335	63Y.65	544.60	.1381	1.0721	2154.68	.3999
63.00	-3.519	636.16	544.60	.1476	1.0746	2159.69	.3999
66.00	-3.707	642.05	544.60	.1572	1.0769	2164.27	.3999
69.00	-3.899	649.12	544.60	.1668	1.0791	2168.67	.3999
72.00	-4.095	655.56	544.60	.1764	1.0813	2173.16	.3999

## DIVERSTION(W) AND TURBULENT(WP) CROSSFLOW BETWEEN ADJACENT SUBCHANNELS (I,J)

CASE 1 SAMPLE PROBLEM FOR COBRA TO ILLUSTRATE INPUT.

DISTANCE	W( 1, 2) WP( 1, 2)	W( 1, 4) WP( 1, 4)	W( 2, 3) WP( 2, 3)	W( 2, 5) WP( 2, 5)	W( 3, 6) WP( 3, 6)
0.00	.0	179.6	.0	179.6	.0
3.00	77.5	224.8	77.5	224.8	177.6
6.00	42.0	279.0	42.0	279.0	132.9
9.00	1.4	300.9	1.4	300.9	218.3
12.00	158.0	275.7	136.0	275.7	87.5
15.00	-125.6	252.0	-125.6	252.0	132.9
18.00	-159.4	300.0	-159.4	300.2	218.3
21.00	-67.6	465.2	-112.4	492.1	87.5
24.00	-29.4	508.8	-40.1	584.7	132.9
27.00	-3.1	640.3	-8.2	646.2	218.3
30.00	10.0	642.8	5.8	646.3	87.5
33.00	15.9	643.4	11.9	645.6	132.9
36.00	14.2	643.3	13.4	644.7	218.3
39.00	44.2	640.2	18.9	657.0	87.5
42.00	20.1	642.0	12.3	651.1	132.9
45.00	17.2	636.2	10.5	640.5	218.3
48.00	15.3	610.3	9.9	612.7	87.5
51.00	10.6	554.0	9.1	585.4	132.9
54.00	5.0	557.5	5.3	558.2	218.3
57.00	48.2	530.5	15.4	545.2	87.5
60.00	25.9	504.4	9.5	514.0	132.9
63.00	15.4	477.0	7.0	482.8	218.3
66.00	11.0	450.2	6.2	453.5	87.5
69.00	8.9	422.5	6.1	424.7	132.9
72.00	7.8	394.0	6.1	396.0	218.3

## DIVERSION(W) AND TURBULENT(WP) CROSSFLOW BETWEEN ADJACENT SUBCHANNELS (I,J)

CASE 1 SAMPLE PROBLEM FOR COBRA TO ILLUSTRATE INPUT.

DISTANCE	W( 4, 5) WP( 4, 5)	W( 4, 7) WP( 4, 7)	W( 5, 6) WP( 5, 6)	W( 5, 8) WP( 5, 8)	W( 6, 9) WP( 6, 9)
.00	.0	177.0	.0	155.7	.0
3.00	132.9	218.3	-6.7	205.5	-42.1
6.00	87.5	272.0	-6.1	254.0	-23.9
9.00	39.7	344.1	-6.2	314.2	-9.4
12.00	61.3	421.6	24.9	377.1	19.9
15.00	-32.2	506.5	-14.9	444.9	-18.0
18.00	-57.7	597.3	1.9	513.6	7.2
21.00	-16.9	675.3	-36.4	577.2	-70.0
24.00	2.1	763.5	.0	629.0	-9.4
27.00	-5.2	860.8	1.9	626.0	-5.1
30.00	-6.2	884.2	2.3	626.2	-4.0
33.00	-6.4	883.4	2.0	627.7	-3.0
36.00	-6.8	883.2	1.5	629.6	-2.9
39.00	24.8	885.4	4.2	641.0	-22.0
42.00	11.9	864.9	5.1	639.4	-14.9
45.00	3.7	864.8	2.9	625.5	-10.7
48.00	-1.2	840.2	11.2	602.0	-8.4
51.00	-1.8	806.5	7.2	578.3	-7.2
54.00	-2.3	772.4	-1.1	554.1	-6.6
57.00	34.4	741.1	.1	538.6	-31.2
60.00	19.8	705.3	2.1	510.7	-21.5
63.00	12.2	669.7	.7	483.5	-15.8
66.00	8.0	634.0	-4.4	456.5	-12.1
69.00	5.9	598.1	-1.4	429.5	-10.1
72.00	5.0	562.0	-2.1	402.4	-9.0

## DIVERSION(W) AND TURBULENT(WP) CROSSFLOW BETWEEN ADJACENT SUBCHANNELS (I,J)

CASE 1 SAMPLE PROBLEM FOR COBRA TO ILLUSTRATE INPUT.

DISTANCE	W( 7, 8) WP( 7, 8)	W( 8, 9) WP( 8, 9)
.00	.0	134.8
3.00	87.2	161.0
6.00	41.7	196.0
9.00	21.8	239.3
12.00	16.6	291.6
15.00	-9.5	348.1
18.00	-1.5	419.7
21.00	27.8	462.4
24.00	11.8	555.4
27.00	3.3	634.3
30.00	.3	661.7
33.00	-1.3	663.3
36.00	-2.2	664.7
39.00	22.0	656.4
42.00	8.6	661.5
45.00	3.1	664.4
48.00	.8	656.4
51.00	.2	632.1
54.00	.0	617.2
57.00	32.6	571.7
60.00	14.2	549.5
63.00	8.3	525.2
66.00	5.3	499.7
69.00	4.0	473.6
72.00	3.5	447.0

APPENDIX F

DISTRIBUTION

DISTRIBUTION

<u>No. of Copies</u>	<u>Offsite</u>
216	AEC Division of Technical <u>Information Extension</u> For UC-80 Distribution
28	AEC Library, Washington <u>Division of Reactor Development Technology</u> Chief, IWOGR Branch Assistant Director, Plant Eng. Chief, Inst. & Cont. Branch Chief, Systems Eng. Branch Chief, Core Design Branch Chief, Fuel Fab, Branch Chief, Control Mech. Br, Asst. Dir., Reactor Tech. Chief, Fuels & Mat, Branch Chief, Reactor Phy. Branch Chief, Special Tech. Branch Asst. Dir., Nuclear Safety Asst. Dir., Program Analysis Water Projects Branch Research and Development Branch R. Feit R. M. Scroggins (2) S. Strauch N. E. Todreas A. Van Echo
	Division of Safety Standards R. Impara
	Office of Assistant General Manager for Reactors Dr, R. C. Dalzell
	Office of Assistant General Counsel for Patents R. A. Anderson
	RDT Site Offices (4)
1	<u>AEC, Chicago Patent Group</u> G. H. Lee
2	<u>Aerojet-General Nucleonics</u> H. Jaffee D. Yee

No. of Copies

1

Allis-Chalmers Manufacturing Company  
Atomic Energy Division  
**6933 Arlington Road**  
P.O. Box 5976  
Bethesda, Maryland 20014

W. S. Fanner

Argonne National Laboratory

Dr. T. R. Bump  
Leonard J. Koch  
Dr. Paul Lottes  
Robert E. Macherey  
M. Noviek  
Dr. M. Petrick  
R. P. Stein

Atomic Energy Commission  
Brussels Office  
U.S. Mission to the European Communities  
APO, New York, N.Y. 09667

2

Atomics International  
P.O. Box 591, Canoga Park, California 91305  
Senior Site Rep., AI-CE  
Acting Senior Site Rep., AI

12

Atomic Energy of Canada, Limited  
Chalk River, Ontario, Canada  
A. Pearson  
G. A. Wikhamer  
Scientific Representative Division  
of International Affairs (10)

2

Atomic Energy Establishment  
Winfrith, Heath, England  
R. W. Bowring  
W. S. Eastwood

2

Atomic Energy Research Establishment  
Harwell, Berkshire, England  
J. G. Collier (nr. Didcot Berkshire)  
G. F. Hewitt

No. of Copies

3      Atomics International  
            Donald T. Eggan  
            David C. Fulton (2)

2      Atomic Power Development Associates, Inc.,  
            Alton P. Donnell

1      Babcock and Wilcox Company  
            Barberton, Ohio  
            P. B. Probert

2      Babcock and Wilcox Company  
            HWOGR Project Manager  
            Donald F. Judd

1      Babcock and Wilcox Company  
            P. O. Box 1260  
            Lynchburg, Virginia 24502  
            R. E. Willard

1      Baldwin-Lima-Hamilton Corporation  
            Industrial Equipment Division  
            Eddystone, Pennsylvania  
            Philip Otten

3      Brookhaven National Laboratory  
            Dr. J. Chen  
            Dr. O. E. Dwyer  
            Dr. David Gurinsky

1      Canadian Westinghouse Co. Ltd.  
            P. O. Box 510  
            Hamilton, Ontario, Canada  
            F. Stern

1      Canadian General Electric  
            P. O. Box 1200  
            Peterborough, Ontario, Canada  
            Dr. J. T. Rogers

No. of Copies

2

Chicago Operations Office

Richard J., Gariboldi

2

Columbia University  
Department of Chemical EngineeringDr. C. F. Bonilla  
J. E. Casterline

4

Combustion Engineering, Inc.HPO, Windsor Representative  
F. Bevilacqua  
Senior Site Representative  
R. C. Noyes

1

Duke Power CompanyP. O. Box 2178  
Charlotte, North Carolina 28201

E. C. Fiss

4

duPont Company, AikenG. Dessauar  
Supervisor, Technical Information Service (2)  
Site Representative, SR

2

duPont Company, WilmingtonDirector, Keactor Engineering Section  
J. S. Neill

1

Dynatech Corporation17 Tudor Street  
Cambridge, Massachusetts 02139

A. Bergles

18

European ContractorsAEG-Kernenergieversuchsanlage  
8752 Grobwlzheim (Unterfranken)  
Germany

Dr. Kirchenmayer (1)

Alstom  
38 Avenue Kleber  
Paris 16e, France

M. P. Domenjoud (1)

No. of  
Copies

ANSALDO  
Direzione Generale (1)  
Piazza Carignano 2  
Genova, Italy

CEN Saclay  
Boite Postale 2  
Gif-Sur-Yvette (S et O), France  
G. Vendryes (10)

Centre d'Etudes Nucleaires  
Chemi des Martyrs  
Grenoble (Isere)  
France

M. Mondin (1)

MAN  
Abholfach  
Nurnberg 2, Germany

Dr, Mayinger (1)

Keactor Centrum Nederland  
112 Scheveningseweg  
\*s gravenhage  
Netherlands

Prof, Dr, M. Bogaardt (1)

SNECMA  
Division Atomique  
22, Quai Gallineni  
Suresnes (Seine)  
France

M. Foure (1)

Technical Hogeschool Eindhoven  
P. O. Box 313  
Eindhoven  
Netherlands

Prof, D. M. Bogaardt (1)

No. of Copies

47

Fast Reactor Technology ExchangeUK/US Fast Reactor Exchange (12)  
EURATOM/US Fast Reactor Exchange (35)Gulf-General Atomic  
P.O. Box 608  
San Diego 12, California 92112

R. Katz

1

General Electric Company, San Jose (Trumbull)  
Advanced Engineering

Karl P. Cohen

3

General Electric Company, San JoseEarl Janssen  
R. T. Lahey  
Dr. S. Levy

2

Georgia Institute of TechnologyJames Rust  
Novak Zuber

1

Geoscience, Ltd.  
La Jolla, California

Dr. H. F. Poppendiek

1

M. W. Kellogg Company  
711 3rd Avenue  
New York 17, New York

B. W. Jesser

1

Jersey Nuclear Corp.  
Bellevue, Washington

L. Torobin

1

Knolls Atomic Power Laboratory  
General Electric Company  
Schenectady, New York

G. H. Halsey

2

Los Alamos Scientific Laboratory

Dr. David B. Hall

No. of Copies

2 Massachusetts Institute of Technology

Dr. P. Griffith  
Dr. W. Rohsenow

1 MSA Research Corporation  
Marketing Division  
Gallery, Pennsylvania 14024

C. H. Staub

6 NASA Lewis Research Center  
Librarian (33)  
J. M. Savino  
R. Weltmann (SEPO) (2)

1 New York Operations Office  
Jules Wise

1 North Carolina State University  
Dr. Z. K. Ferrell

1 Nuclear Materials & Equipment Corp.  
Zalman M. Shapiro

1 NUS Corporation  
Idaho Falls, Idaho  
G. A. Freund

1 Nuclear Technology Corporation  
116 Main Street  
White Plains, New York 10601  
F. R. Hubbard

2 Oregon State University  
Dr. J. G. Knudsen  
Dr. J. R. Welty

1 Power Reactor Development Company  
1911 First Street  
Detroit, Michigan 48226  
Arthur S. Griswold

No. of  
Copies

1      Purdue University  
          Mechanical Engineering Department  
          P. W. McFadden

1      Rutgers University  
          R. L. Peskin

1      Southwest Atomic Energy Associates  
          Post Office Box 1106  
          Shreveport, Louisiana 71102

1      Stanford University  
          Dr. G. Leppert

1      TRW Space Technology Laboratories  
          TRW Systems Group  
          S. M. Zivi

2      Union Carbide Corporation (ORNL)  
          Dr. Floyd L. Culler (2)

2      Union Carbide Corp. (ORNL-Y-12)  
          W. R. Gambill  
          H. W. Hoffman

2      United Nuclear Corporation  
          Grasslands Road  
          Elmsford, New York  
          R. W. Carlson  
          Alred Strasser

2      University of Michigan (VESIAC)  
          Dept. of Chemical and Met. Engineering  
          R. Balzhiser  
          J. A. Clark

1      University of Minnesota  
          Department of Chemical Engineering  
          Minneapolis, Minnesota 55455  
          H. S. Isbin

No. of Copies

2	<u>University of Washington</u> C. J. Kippenhan R. W. Moulton
2	<u>Westinghouse Bettis Atomic Power Laboratory</u> S. Green (2)
2	<u>Westinghouse Electric Corporation</u> R. Solbrig L. S. Tong
1	<u>Washington State University</u> Dr. John Lienhard
	<u>Onsite--Hanford</u>
1	<u>AEC, Chicago Patent Group</u> R. K. Sharp
1	<u>AEC, RL</u> C. L. Robinson
2	<u>AEC, RDT Site Representative</u> P. G. Holsted
3	<u>Battelle Memorial Institute</u>
7	<u>Douglas United Nuclear</u> P. A. Carlson H. R. Kosmata R. H. Shoemaker File--4
111	<u>Battelle-Northwest</u> F. W. Albaugh R. T. Allemand J. K. Anderson C. W. Angle E. R. Astley J. M. Batch A. L. Bement

No. of  
CopiesBattelle-Northwest (Continued)

G. J. Busselman  
J. J. Cadwell  
N. E. Carter  
P. D. Cohn  
D. L. Condotta  
G. M. Dalen  
F. G. Dawson  
R. L. Dillon  
E. A. Eschbach  
J. R. Fishbaugher  
D. E. Fitzsimmons  
G. L. Fox  
J. C. Fox  
M. D. Freshley  
S. Goldsmith  
W. L. Hampson  
H. E. Hanthorn  
R. A. Harvey  
G. M. Hesson  
R. M. Hiatt  
B. M. Johnson  
R. L. Junkins  
D. C. Kolesar  
C. E. Leach  
W. R. Lewis  
C. W. Lindenmeier  
T. I. McSweeney  
M. K. Millhollen  
C. A. Oster  
A. Padilla  
L. T. Pedersen  
R. E. Peterson  
R. H. Purcell  
T. C. Reihman  
W. E. Roake  
G. J. Rogers  
D. S. Rowe (SO)  
A. M. Sutey  
W. L. Thorne  
R. E. Turley  
P. C. Walkup  
C. L. Wheeler  
R. G. Wheeler  
K. R. wise

No, of  
Copies

Battelle-Northwest (Continued)

N. G. Wittenbrock  
W. C. Wolkenhauer  
J. M. Yatabe  
F. R. Zaloudek  
Technical Information Files (5)  
Technical Publications (2)